The Journal of Physiology

Promotion of endocytosis efficiency through an ATP-independent mechanism at rat calyx of Held terminals

Hai-Yuan Yue[1], Erhard Bieberich[1] and Jianhua Xu[1,2]

[1] *Departments of Neuroscience and Regenerative Medicine, Augusta University, USA*
[2] *Department of Neurology, Medical College of Georgia, Augusta University, USA*

Key points

- At rat calyx of Held terminals, ATP was required not only for slow endocytosis, but also for rapid phase of compensatory endocytosis.
- An ATP-independent form of endocytosis was recruited to accelerate membrane retrieval at increased activity and temperature.
- ATP-independent endocytosis primarily involved retrieval of pre-existing membrane, which depended on Ca^{2+} and the activity of neutral sphingomyelinase but not clathrin-coated pit maturation.
- ATP-independent endocytosis represents a non-canonical mechanism that can efficiently retrieve membrane at physiological conditions without competing for the limited ATP at elevated neuronal activity.

Abstract Neurotransmission relies on membrane endocytosis to maintain vesicle supply and membrane stability. Endocytosis has been generally recognized as a major ATP-dependent function, which efficiently retrieves more membrane at elevated neuronal activity when ATP consumption within nerve terminals increases drastically. This paradox raises the interesting question of whether increased activity recruits ATP-independent mechanism(s) to accelerate endocytosis at the same time as preserving ATP availability for other tasks. To address this issue, we studied ATP requirement in three typical forms of endocytosis at rat calyx of Held terminals by whole-cell membrane capacitance measurements. At room temperature, blocking ATP hydrolysis effectively abolished slow endocytosis and rapid endocytosis but only partially inhibited excess endocytosis following intense stimulation. The ATP-independent endocytosis occurred at calyces from postnatal days 8–15, suggesting its existence before and after hearing onset. This endocytosis was not affected by a reduction of exocytosis using the light chain of botulinum toxin C, nor by block of clathrin-coat maturation. It was abolished by EGTA, which preferentially blocked endocytosis of retrievable membrane pre-existing at the surface, and was impaired by oxidation of cholesterol and inhibition of neutral sphingomyelinase. ATP-independent endocytosis became more significant at 34–35°C, and recovered membrane by an amount that, on average, was close to exocytosis. The results of the present study suggest that activity and temperature recruit ATP-independent endocytosis of pre-existing membrane (in addition to ATP-dependent endocytosis) to efficiently retrieve membrane at nerve terminals. This less understood endocytosis represents a non-canonical mechanism regulated by lipids such as cholesterol and sphingomyelinase.

(Resubmitted 4 March 2017; accepted after revision 15 May 2017; first published online 29 May 2017)
Corresponding author J. Xu: Medical College of Georgia, Augusta University, 1120 15th Street, CA 3010, Augusta, GA 30912, USA. Email: jxu1@augusta.edu

Abbreviations aCSF, artificial cerebrospinal fluid; AMP-PNP, adenosine 5′-(β,γ-imido)triphosphate lithium salt hydrate; Cm, membrane capacitance; COase, cholesterol oxidase; nSMase, neutral sphingomyelinase; SMase, sphingomyelinase.

 DOI: 10.1113/JP274275

Introduction

At nerve terminals, endocytosis immediately follows exocytosis to recycle the vesicle membrane for sustaining neurotransmission during repetitive activity, as well as to maintain membrane homeostasis. Endocytosis kinetics depends on neuronal activity and Ca^{2+}. Most membrane capacitance measurements have revealed two kinetically different endocytosis pathways, slow endocytosis with a time constant (τ) of a few to tens of seconds and rapid endocytosis (τ of ~2 s), at large synapses such as retina bipolar cells (von Gersdorff & Matthews, 1994; Neves & Lagnado, 1999; Jockusch *et al.* 2005), hair cells (Beutner *et al.* 2001; Neef *et al.* 2014) and the calyx of Held (Wu *et al.* 2005; Lou *et al.* 2008). Both pathways contribute to compensatory endocytosis following regular stimulation. In addition, very rapid, excess endocytosis that retrieves more membrane than newly fused has been observed at synapses following intense stimulation (Wu *et al.* 2009; Xue *et al.* 2012; Okamoto *et al.* 2016), large Ca^{2+} transient (Beutner *et al.* 2001) and at physiological temperature (Renden & von Gersdorff, 2007). At small synapses such as hippocampal boutons, imaging of vesicular membrane cargoes attached to pH-sensitive fluorescent proteins demonstrates primarily slow endocytosis with τ of seconds to tens of seconds (Armbruster & Ryan, 2011), which remains rather constant at different levels of activity (Sankaranarayanan & Ryan, 2000; Kononenko *et al.* 2014). However, because the temporal resolution of this method is limited by the rate of vesicle acidification and sampling interval, endocytosis with τ of ~2 s, if present, could have escaped detection (Kononenko & Haucke, 2015; Okamoto *et al.* 2016). Indeed, imaging with quantal dots and high-pressure freezing electron microscopy have demonstrated that hippocampal boutons contain the rapid 'kiss-and-run' mode of endocytosis (Zhang *et al.* 2009) and ultrafast endocytosis with τ < 100 ms (Watanabe *et al.* 2013). Rapid endocytosis has also been reported based on imaging with fluorescent styryl dyes (Maeno-Hikichi *et al.* 2011). In general, activity increases the absolute rate of membrane endocytosis to efficiently reverse the membrane expansion upon exocytosis (Wu *et al.* 2009; Maeno-Hikichi *et al.* 2011), probably as a result of acceleration of an existing pathway, switching to a faster mechanism, and/or recruitment of additional pathway(s). Activity controls the participation of a given mechanism (e.g. clathrin-mediated endocytosis) (Granseth *et al.* 2006; Kononenko *et al.* 2014). Numerous studies have indicated that slow endocytosis is mainly mediated by clathrin and the GTP-dependent dynamin (Yamashita *et al.* 2005; Granseth *et al.* 2006; Newton *et al.* 2006; Lou *et al.* 2008; Xu *et al.* 2008; Hosoi *et al.* 2009; Wu *et al.* 2009). The rapid component of compensatory endocytosis depends on GTP hydrolysis and probably dynamin (Xu *et al.* 2008) but not clathrin (Jockusch *et al.* 2005). The overshoot of excess endocytosis also involves Ca^{2+} (Renden & von Gersdorff, 2007; Wu *et al.* 2009), calmodulin (Wu *et al.* 2009), calcineurin, GTP and dynamin (Xue *et al.* 2012) but not clathrin (Yue & Xu, 2015). Clarification of the activity-dependent selection of endocytic mechanisms is important for understanding synaptic functions.

Endocytosis in synapses has been reported to depend on ATP (Heidelberger, 2001; Rangaraju *et al.* 2014; Pathak *et al.* 2015; but see also Van Hook & Thoreson, 2012). Meanwhile, neuronal activity can stimulate many other ATP-dependent processes, such as action potential firings, vesicle mobilization and priming, vesicle reacidification, and Ca^{2+} clearance, which may account for rapid depletion of intracellular ATP (Rangaraju *et al.* 2014). The paradox between ATP stress and accelerated endocytosis raises the question of whether terminals during increased activity utilize ATP-independent mechanisms to facilitate endocytosis without jeopardizing ATP availability for other tasks. In addition, depletion of ATP impairs endocytosis much more potently than block of an ATP-dependent process, such as actin polymerization (Wu *et al.* 2016) and clathrin-uncoating (Yim *et al.* 2010), implying that endocytosis requires ATP in multiple steps. Alternatively, ATP is essential for a key endocytic step. At *Drosophila* nerve terminals, nucleoside diphosphate kinase has been reported to rely on ATP for converting GDP into GTP, which is needed for the functions of dynamin (Krishnan *et al.* 2001). Blockade of GTP hydrolysis can abolish slow and rapid compensatory endocytosis (Yamashita *et al.* 2005; Xu *et al.* 2008). Whether ATP requirement in endocytosis at mammalian central synapses is linked to GTP-dependence has not been tested.

To address these questions, we investigated ATP-dependence of endocytosis at rat calyx of Held terminals using whole-cell membrane capacitance (Cm) measurements. We found that ATP was required for both rapid and slow endocytosis but not for endocytosis of pre-existing membrane, which significantly contributed to endocytosis at elevated activity and temperature. ATP-independent endocytosis was impaired by cholesterol oxidation and inhibition of sphingomyelinase but not inhibition of exocytosis or clathrin-coat maturation. The results of the present study highlight the importance of a non-canonical, ATP-independent mechanism in endocytosis at nerve terminals.

Methods

Ethical approval

Sprague–Dawley rats were initially purchased from Envigo (Indianopolis, IN, USA) and later bred inhouse. Animals had been attended and used in accordance with procedures approved by the Institutional Animal Care and Use

Committee of Augusta University (#2011-0347). This study complied with the animal ethical principles that *The Journal of Physiology* operates under (Grundy, 2015).

Slice preparation

Male and female Sprague–Dawley rat pups were acutely decapitated without anaesthesia [8–11 days old, i.e., post-natal day (P)8–11] or after anaesthesia (14–15 days old, P14–15) in acordance with procedures approved by Institutional Animal Care and Use Committee of Augusta University. Specifically, anaesthesia was induced inside a Biosafety Level 2 cabinet by applying iso-fluorane (0.3 ml rat^{-1}) to cotton near the rat in a jar with a tight fitting lid. Parasagittal brainstem slices (160–200 μm thick) were sectioned using an automated VT1200S slicer (Leica Microsystems, Wetzlar, Germany) in ice-cold low-Ca^{2+} artificial cerebrospinal fluid (aCSF), which contained (in mM): 125 NaCl, 25 $NaHCO_3$, 2.5 KCl, 1.25 NaH_2PO_4, 3 $MgCl_2$, 0.5 $CaCl_2$, 25 glucose, 0.4 Na ascorbate, 3 myo-inositol and 2 Na pyruvate, and was bubbled with 95% O_2 and 5% CO_2. Slices were transferred into normal aCSF to recover for 45 min at 37°C. The normal aCSF was identical to the low-Ca^{2+} aCSF except that it contained 1 mM $MgCl_2$ and 2 mM $CaCl_2$. After recovery, slices were kept at room temperature (22–24°C).

Membrane capacitance measurement

Brain slices were transferred to a recording chamber and constantly perfused with a bath solution containing (in mM): 105 NaCl, 20 TEA-Cl, 2.5 KCl, 1 $MgCl_2$, 25 $NaHCO_3$, 1.25 NaH_2PO_4, 25 glucose, 0.4 Na ascorbate, 3 myo-inositol, 2 Na pyruvate, 0.001 tetrodotoxin and 0.1 3,4-diaminopyridine, and bubbled with 95% O_2 and 5% CO_2. The bath solution also contained 2 mM $CaCl_2$ or 6 mM $CaCl_2$ as indicated. We visually identified the calyx terminals and performed the whole-cell, patch clamp technique with an EPC-10/2 amplifier controlled by Patchmaster (HEKA, Lambrecht, Germany). The control pipette solution contained (in mM): 125 Cs-gluconate, 20 CsCl, 4 MgATP, 10 Na_2-phosphocreatine, 0.3 GTP, 10 Hepes and 0.05 BAPTA, and was adjusted to pH 7.2 with CsOH. To monitor exocytosis and endocytosis by Cm measurement in real time, the calyx terminals were voltage clamped at −80 mV with a 1 kHz, 60 mV peak-to-peak sinusoidal wave superimposed (Lindau & Neher, 1988; Sun & Wu, 2001). Data points of Cm were sampled at 1 kHz without averaging. If not indicated otherwise, we evoked exocytosis and endocytosis from terminals > 4 min after whole-cell recording, by applying single or repetitive depolarization pulses of 1, 20 and 50 ms, respectively. As indicated, the pipette solution was added with ATPγS (EMD Millipore Chemicals, Darmstadt, Germany), the light chain of botulinum toxin C (List Biological Lab., Campbell, CA, USA), Pitstop 1 (Abcam, Cambridge, MA, USA), an AP2-blocking peptide containing the DNF motif of amphiphysin-1 (DNF peptide: INFFEDNFVPEI; 21st Century Biochemicals, Marlborough, MA, USA), adenosine 5′-(β,γ-imido)triphosphate lithium salt hydrate (AMP-PNP), sphingomyelinase from *Bacillus cereus* (SMase; catalogue number S7651), cholesterol oxidase (COase), EGTA (Sigma-Aldrich, St Louis, MO, USA), spiroepoxide or sphingolactone-24 (Santa Cruz Biotechnology, Santa Cruz, CA, USA). Recordings were made at either 22–24°C (Figs 1–6) or 34–35°C (Figs 7–9).

Data analysis

If not otherwise indicated, we only analysed Ca^{2+} channel current, exocytosis and endocytosis induced by the first stimulation from each calyx, such that the results are not confounded by depletion of pre-existing membrane during preceding stimulation, or reduction of Ca^{2+} current and exocytosis upon subsequent stimulation in the block of ATP hydrolysis. We evaluated the inhibitory effects on endocytosis by comparison of the initial rate of endocytosis ($Rate_{endo}$) and the amount of endocytosis. $Rate_{endo}$ was calculated from linear fitting of Cm decay within 2 s after stimulation with a train of ten 20–50 ms pulses or 20 brief (1 ms) pulses, or within 4 s after stimulation with a 20 ms pulse or 500 brief pulses. To reflect consequence in membrane recovery, we measured the amount of Cm decay at either 25 s ($Endo_{25s}$) or 45 s ($Endo_{45s}$) after different stimulation paradigms, when endocytosis largely completed in control. Data are reported as the mean ± SEM from nerve terminals (n = 5–11) and were analysed by one-way ANOVA followed by a *post hoc* Tukey's test for significance levels of difference ($^{*}P < 0.05$ and $^{**}P < 0.01$ between control and treatment, respectively).

Results

Co-existence of ATP-dependent and ATP-independent endocytosis

Whole-cell capacitance measurements at the calyx of Held have revealed three common endocytosis mechanisms (i.e. slow endocytosis, rapid endocytosis and excess endocytosis) following different stimulation paradigms (Wu *et al.* 2005; Renden & von Gersdorff, 2007; Wu *et al.* 2009; Yamashita *et al.* 2010; Xue *et al.* 2012). Whether these mechanisms differentially require ATP has not been investigated. We set out to solve this issue as described below.

First, we examined slow endocytosis induced by a prolonged depolarization pulse from −80 mV to 0 mV for 20 ms (referred to as $depol_{20ms}$) at calyces perfused by

solution containing 2 mM Ca^{2+}. At calyces dialysed with control pipette solution containing 4 mM ATP, stimulation with $depol_{20ms}$ evoked a sharp Cm increase (ΔCm) of 443 ± 20 fF ($n = 7$) (Fig. 1*A* and *B* and Table 1), followed by mono-exponential Cm decline to the baseline ($\tau = 14.9 \pm 1.2$ s). Because Cm is proportional to the area of plasma membrane, ΔCm and Cm decay correspond to exocytosis and endocytosis at calyces, respectively (Sun & Wu, 2001). Endocytosis had an initial rate ($Rate_{endo}$) of 30 ± 3 fF s^{-1} and summed up to 378 ± 19 fF at 25 s after $depol_{20ms}$ ($Endo_{25s}$). To test its requirement for ATP, we examined calyces dialysed for > 4 min with the pipette solution containing 4 mM ATPγS or AMP-PNP instead of ATP. ATPγS reduced exocytosis to 307 ± 33 fF ($P < 0.01$, $n = 7$) and blocked endocytosis ($Rate_{endo} = 3 \pm 2$ fF s^{-1} and $Endo_{25s} = 25 \pm 12$ fF, $P < 0.01$), leaving ~90% of membrane expansion during exocytosis unrestored. Impairment of endocytosis by ATPγS was not caused by reduction of Ca^{2+} current, which did not happen during the first stimulation that we analysed (Fig. 1*B*). AMP-PNP

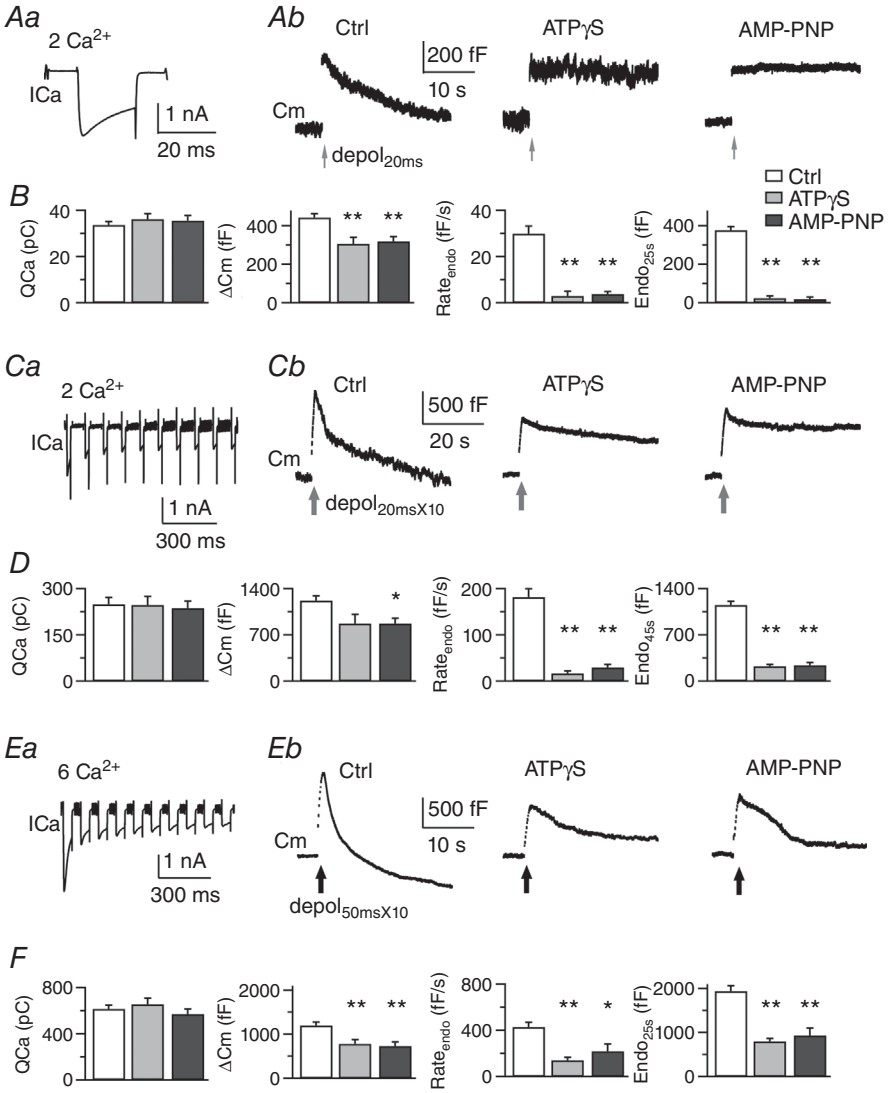

Figure 1. ATP-dependent and ATP-independent mechanisms co-exist at the calyx of Held terminals
A, sampled Ca^{2+} channel current from a control calyx (ICa, *Aa*) and membrane capacitance responses (Cm, *Ab*) following $depol_{20ms}$ under dialysis with the control pipette solution (Ctrl), 4 mM ATPγS or 4 mM AMP-PNP, respectively. Bath Ca^{2+} was 2 mM. *B*, summary of charge of ICa (QCa), exocytosis (ΔCm), initial rate of endocytosis ($Rate_{endo}$) and membrane retrieved at 25 s ($Endo_{25s}$) induced by $depol_{20ms}$ for control ($n = 7$), ATPγS ($n = 7$) and AMP-PNP ($n = 6$). Colour code for treatments also applies to (*D*) and (*F*). *C* and *D*, sampled ICa from a control calyx (*Ca*) and Cm responses (*Cb*) induced by $depol_{20msX10}$ at calyces bathed in 2 mM Ca^{2+}. Summarized data are from calyces dialysed with control pipette solution ($n = 7$), ATPγS ($n = 7$) and AMP-PNP ($n = 5$), respectively. *E* and *F*, sampled ICa from a control calyx (*Ea*) and Cm responses (*Eb*) induced by $depol_{50msX10}$ at calyces bathed in 6 mM Ca^{2+}. Summarized data are from control ($n = 8$), ATPγS ($n = 9$) and AMP-PNP ($n = 9$), respectively.

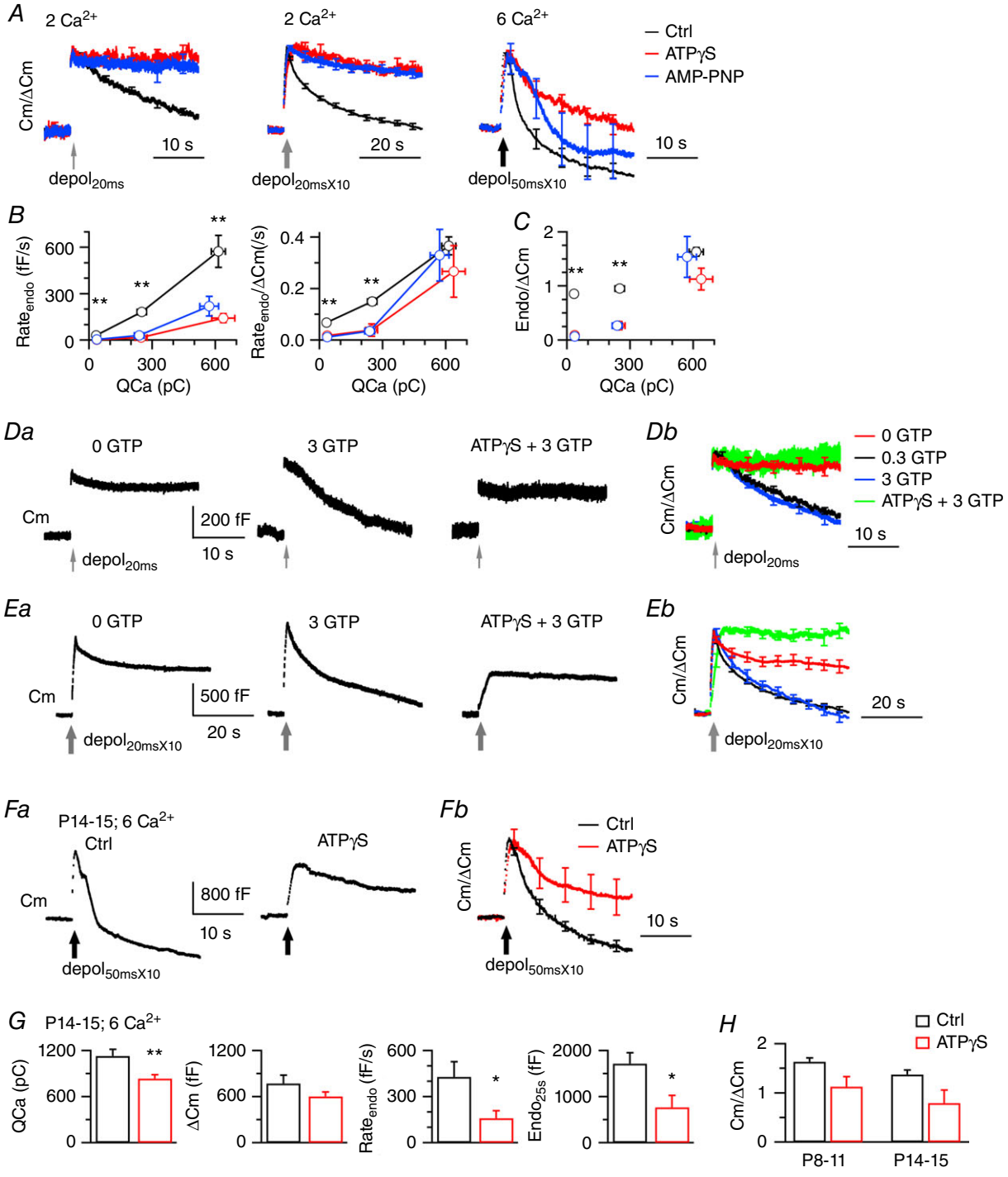

Figure 2. ATP-independent endocytosis is facilitated by activity/Ca^{2+} and is independent of GTP or the development of calyces

A, average Cm responses after normalization to exocytosis (ΔCm) are superimposed for comparison of endocytosis kinetics. Error bars are SEM. Original data in (*A*) to (*C*) are from tests in Fig. 1*Ab*, *Cb* and *Eb*. Colour code of treatments also applies to (*B*) and (*C*). *B*, $Rate_{endo}$, or $Rate_{endo}$ normalized to exocytosis (ΔCm), was plotted against QCa induced by $depol_{20ms}$, $depol_{20msX10}$ and $depol_{50msX10}$, respectively. Ca^{2+} increases initial rate of endocytosis, with the contribution of the ATP-independent pathway obviously detected for $depol_{50msX10}$ that induced QCa of ∼600 pC. **Statistically significant difference ($P < 0.01$) between control and ATPγS or AMP-PNP ($n = 5$–9), which applies to (*C*). *C*, amount of membrane retrieval normalized to ΔCm *vs.* QCa. Note that with Ca^{2+} influx of ∼600 pC, ATP-independent endocytosis and control endocytosis recovered a similar percentage of membrane with respective to exocytosis. *D* and *E*, sampled Cm responses by either $depol_{20ms}$ or $depol_{20msX10}$

from calyces dialysed with no GTP, 3 mM GTP, or 4 mM ATPγS (replacing ATP) and 3 mM GTP, respectively. Bath Ca^{2+} was 2 mM. Average Cm traces after normalization to ΔCm are superimposed (*Db* and *Eb*) to compare endocytosis kinetics. Each test condition includes five to eight calyces. *F*, sampled (*Fa*) and average (*Fb*) Cm responses to $depol_{50msX10}$ from P14–15 calyces dialysed with the standard (Ctrl) or 4 mM ATPγS solution. Bath Ca^{2+} was 6 mM. *G*, summarized data from P14–15 calyces of Ctrl ($n = 5$) and ATPγS ($n = 6$). Compared to data from P8–11 calyces (Fig. 1*E–F*), QCa was larger ($P < 0.01$ in Ctrl and $P < 0.05$ in ATPγS). ΔCm, $Rate_{endo}$ and $Endo_{25s}$ were similar between age groups. *H*, ATP-independent endocytosis accounted for 68 ± 12% and 58 ± 18% in excess endocytosis induced by $depol_{50msX10}$ at calyces from P8–11 and P14–15 rats, respectively. It recovered membrane equivalent to ≥79% of exocytosis (ΔCm) in both age groups. Statistics with a *t* test indicate no significant differences between age groups ($P = 0.07$ for Ctrl).

caused similar effects as ATPγS (Fig. 1*A* and *B*), indicating that slow endocytosis following $depol_{20ms}$ depends on ATP hydrolysis, and not protein activation via ATP-binding.

Second, we studied rapid endocytosis following ten repetitive $depol_{20ms}$ delivered at 10 Hz (referred to as $depol_{20msX10}$) (Fig. 1*C* and *D*). In control, $depol_{20msX10}$ induced ΔCm of 1223 ± 71 fF ($n = 7$), followed by initial rapid endocytosis ($\tau = 1.8 \pm 0.1$ s, 30 ± 2%; $Rate_{endo} = 182 \pm 18$ fF s^{-1}) and later slow endocytosis ($\tau = 19.4 \pm 1.1$ s). Dialysis with ATPγS or AMP-PNP did not change Ca^{2+} influx for the first $depol_{20msX10}$, but reduced exocytosis to 876 ± 138 fF ($n = 7$, $P = 0.052$) or 875 ± 80 fF ($n = 5$, $P < 0.05$). ATPγS and AMP-PNP removed the initial rapid endocytosis, reducing $Rate_{endo}$ to 17 ± 5 fF s^{-1} and 30 ± 7 fF s^{-1}, respectively. Membrane recovery within 45 s after $depol_{20msX10}$ was 228 ± 30 fF for ATPγS ($P < 0.01$ *vs.* 1153 ± 58 fF in control) and 244 ± 43 fF for AMP-PNP ($P < 0.01$). These results indicate strong inhibition of both rapid and slow endocytosis by ATPγS or AMP-PNP.

Third, as in previous studies (Wu *et al.* 2009; Yue & Xu, 2015), we induced excess endocytosis by applying ten 50 ms pulses every 50 ms (referred to as $depol_{50msX10}$) to calyces perfused with 6 mM Ca^{2+} (Fig. 1*E* and *F* and Table 1). In control, $depol_{50msX10}$ evoked bi-exponential endocytosis ($\tau = 2.3 \pm 0.4$ s and 13.5 ± 3.2 s, $n = 8$), which was initially very fast ($Rate_{endo} = 430 \pm 41$ fF s^{-1}) and exceeded exocytosis (ΔCm = 1199 ± 80 fF) by an overshoot of 741 ± 90 fF at 25 s after $depol_{50msX10}$. Dialysis with ATPγS inhibited exocytosis (784 ± 99 fF, $P < 0.01$, $n = 9$) and endocytosis ($Rate_{endo} = 141 \pm 25$ fF s^{-1}, $P < 0.01$; $\tau = 9.2 \pm 1.9$ s, range 2.0–18.9 s). The overshoot was not seen at 5 calyces (Fig. 1*Eb*) but occurred at four other calyces (178–452 fF, not shown). The average membrane retrieval, $Endo_{25s}$, was 796 ± 69 fF ($P < 0.01$ *vs.* 1939 ± 125 fF in control). AMP-PNP caused similar inhibition of exocytosis (735 ± 91 fF, $P < 0.01$, $n = 9$) and endocytosis ($Rate_{endo} = 219 \pm 63$ fF s^{-1}, $P < 0.05$; $\tau = 7.3 \pm 1.4$ s, range 2.7–13.7 s). An overshoot of 224–1384 fF appeared at five out of nine calyces, whereas the average $Endo_{25s}$ decreased to 935 ± 169 fF ($P < 0.01$). Thus, both ATPγS and AMP-PNP inhibited only part of excess endocytosis following $depol_{50msX10}$.

The above results have revealed activity-dependent efficacies of ATPγS or AMP-PNP in blocking endocytosis. By averaging Cm changes after normalization to exocytosis (ΔCm), we find that ATPγS and AMP-PNP blocked almost all the membrane recovery following $depol_{20ms}$, prevented most of the membrane recovery following $depol_{20msX10}$, and inhibited excess endocytosis following $depol_{50msX10}$ so that the average endocytosis was close to exocytosis (Fig. 2*A–C*). Because these three forms of endocytosis at the calyx strongly depend on GTP (Yamashita *et al.* 2005; Xu *et al.* 2008; Xue *et al.* 2012), we tested whether they require ATP for regenerating GTP as in *Drosophila* nerve terminals (Krishnan *et al.* 2001). The results obtained suggest that impairment of endocytosis by ATPγS or AMP-PNP was not caused by acute reduction of GTP generation from ATP. First, compensatory endocytosis recorded with the standard pipette solution containing 0.3 mM GTP had both rapid (~2 s) and slow (< 20 s) time constants, which are not slower than optical measurements (up to tens of seconds) at intact synapses (Granseth *et al.* 2006; Hua *et al.* 2011; Pan *et al.* 2015). Increasing GTP in the pipette solution to 3 mM did not further speed up endocytosis, whereas removing GTP severely impaired endocytosis (Fig. 2*D* and *E* and Table 1). Thus, the exogenous GTP (0.3 mM) supplied via the pipette not only is required, but also is sufficient to support normal endocytosis at terminals under whole-cell, patch clamp recordings. Conversion from ATP to GTP should have little impact on endocytosis in our acute tests. Second, supplying 3 mM GTP along with ATPγS did not rescue the endocytosis block (Fig. 2*D* and *E* and Table 1). Therefore, independent of GTP requirement, ATP hydrolysis is essential for the rapid and slow forms of compensatory endocytosis induced by $depol_{20ms}$ and $depol_{20msX10}$, and for a part of excess endocytosis following $depol_{50msX10}$.

Interestingly, ATPγS and AMP-PNP became less efficacious in blocking endocytosis induced by intense stimulation or large Ca^{2+} influx. For example, $Rate_{endo}$ at calyces dialysed with ATPγS was 3 fF s^{-1} after $depol_{20ms}$, 17 fF s^{-1} after $depol_{20msX10}$ and 141 fF s^{-1} after $depol_{50msX10}$ (Figs 1 and 2), which showed an up to 47-fold difference. Dialysis with AMP-PNP led to similar $Rate_{endo}$ after each stimulation (Figs 1 and 2). These results indicate that, in addition to ATP-dependent endocytosis, activity inducing large Ca^{2+} influx (Fig. 2*B* and *C*) can recruit ATP-independent mechanism(s) to

retrieve membrane efficiently. Furthermore, at mature calyces from P14–15 rats after hearing onset, depol$_{50msX10}$ similarly induced excess endocytosis at control, which was partially inhibited by ATPγS (Fig. 2*F*–*H*). At 25 s after depol$_{50msX10}$, ATP-independent endocytosis was 767 ± 261 fF (n = 6), which is equivalent to 79 ± 26% of exocytosis (1003 ± 98 fF). Therefore, the ATP-independent mechanism contributes to endocytosis not only at immature calyces, but also at mature calyces.

ATP-independent endocytosis retrieves pre-existing membrane

We observed that both ATP-dependent and ATP-independent mechanisms contributed significantly to endocytosis following depol$_{50msX10}$, which induces excess endocytosis in control. Because excess endocytosis retrieves more membrane than exocytosis, it contains contribution from a pool of retrievable membrane pre-existing at the surface (Hua *et al.* 2011;

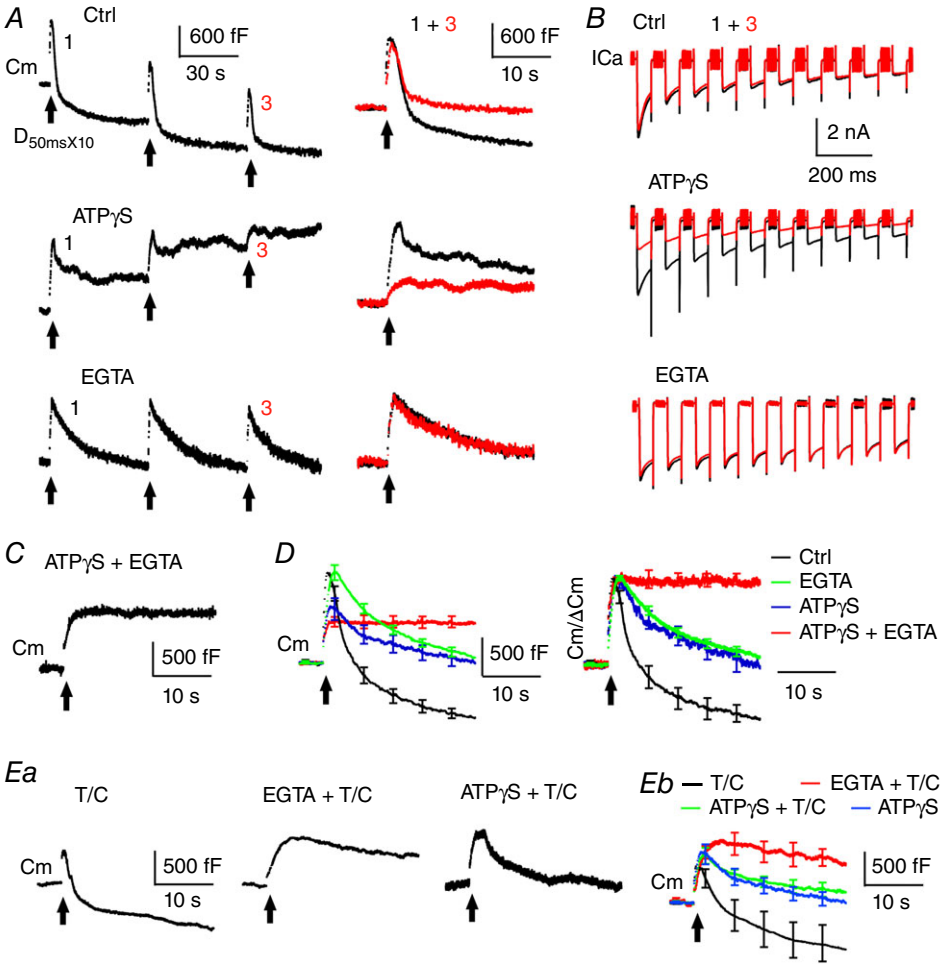

Figure 3. ATP-independent endocytosis is correlated with endocytosis of pre-existing membrane
A, left: sampled Cm responses to three consecutive depol$_{50msX10}$ recorded at calyces under dialysis with control pipette solution, 4 mM ATPγS or 20 mM EGTA. Right: Cm responses to the first and third depol$_{50msX10}$ are superimposed to demonstrate depression of endocytosis in control and ATPγS but not in EGTA. EGTA blocked depression by preventing use-dependent depletion of pre-existing membrane over stimulation. Bath solution contained 6 mM Ca^{2+} for all experiments. *B*, sampled ICa recordings evoked by the first and third depol$_{50msX10}$. Note that ATPγS did not affect ICa during initial pulses but reduced ICa during subsequent pulses and trains. *C*, sampled Cm responses to depol$_{50msX10}$ recorded at a calyx under dialysis with ATPγS and EGTA. *D*, average Cm traces without (left) and with normalization to ΔCm (right). Both ATPγS and EGTA partially inhibited endocytosis induced by depol$_{50msX10}$, whereas their co-dialysis abolished endocytosis. Only responses to the first depol$_{50msx10}$ are analysed. *E*, sampled Cm responses to depol$_{50msX10}$ recorded from calyces under dialysis with the light chain of botulinum toxin C (T/C, 0.5 μM), EGTA and T/C, or ATPγS and T/C. *Eb*, average Cm traces from these treatments are superimposed. Error bars indicate the SEM. Note that T/C reduced exocytosis and thus highlighted endocytosis of pre-existing membrane, which is blocked by EGTA but not ATPγS. Each test condition contains five to nine calyces.

Xue *et al.* 2012). We next examined the possibility that ATP-dependent and ATP-independent mechanisms could selectively retrieve pre-existing membrane and newly fused membrane, respectively.

To determine whether a partial inhibition of excess endocytosis induced by $depol_{50msX10}$ is targeted at pre-existing membrane, we initially adopted an assay measuring the difference of endocytosis following consecutive stimulation (Xue *et al.* 2012). When 3–4 $depol_{50msX10}$ was applied in the presence of 6 mM bath Ca^{2+}, endocytosis at control calyces (P8–11) decreased over repeated stimulation, leading to little overshoot upon the third or fourth $depol_{50msX10}$ (Fig. 3*A*). Because the endocytic depression results from use-dependent depletion of pre-existing membrane by prior $depol_{50msX10}$ (Xue *et al.* 2012), the difference between Cm decay after the first and the third $depol_{50msX10}$ (Fig. 3*A*, right) provides a rough measurement of pre-existing membrane retrieved by the first $depol_{50msX10}$ (Xue *et al.* 2012). This amount was 798 ± 138 fF in control ($n = 8$). Dialysis with ATPγS reduced exocytosis but did not change the pattern of endocytosis depression or the difference of Cm decay between the first and the third $depol_{50mxX10}$ (824 ± 151 fF, $n = 7$). This result implies that ATPγS does not affect use of pre-existing membrane during endocytosis. However, ATPγS reduced Ca^{2+} influx upon the third $depol_{50msX10}$ by half (QCa = 332 ± 33 pC *vs.* 637 ± 55 pC for the first $depol_{50msX10}$) (Fig. 3*B*), which by itself could inhibit endocytosis over stimulation (Fig. 2*B* and *C*) and thus affect our conclusion using this assay (Xue *et al.* 2012). Therefore, we designed two new methods to identify which membrane source underlies ATP-independent endocytosis.

First, we took advantage of the Ca^{2+} chelator, EGTA. As in a previous study (Wu *et al.* 2009), dialysis with 20 mM EGTA inhibited endocytosis following $depol_{50msX10}$ ($Rate_{endo} = 183 \pm 27$ fF s^{-1}; $\tau = 10.3 \pm 1.5$ s, $n = 9$) (Fig. 3*A* and *D*) and prevented retrieval of excess membrane (ΔCm = 1348 ± 74 fF and $Endo_{25s}$ = 1201 ± 87 fF) (Table 1). Interestingly, repetitive $depol_{50msX10}$ evoked almost identical endocytosis (Fig. 3*A*), with $Endo_{25s}$ of 1172 ± 79 fF ($n = 6$) for the third $depol_{50msX10}$. Ca^{2+} influx was also stable (Fig. 3*B*). QCa was 884 ± 48 pC and 907 ± 58 pC for the first and third $depol_{50msX10}$, respectively. This new information indicates that EGTA prevents consumption and thus use-dependent depletion of pre-existing membrane. When EGTA and ATPγS were simultaneously dialysed into calyces, endocytosis became extremely slow ($Rate_{endo} = 6 \pm 3$ fF s^{-1}, $n = 6$) (Fig. 3*C*–*E*) and retrieved membrane by only 59 ± 15 fF

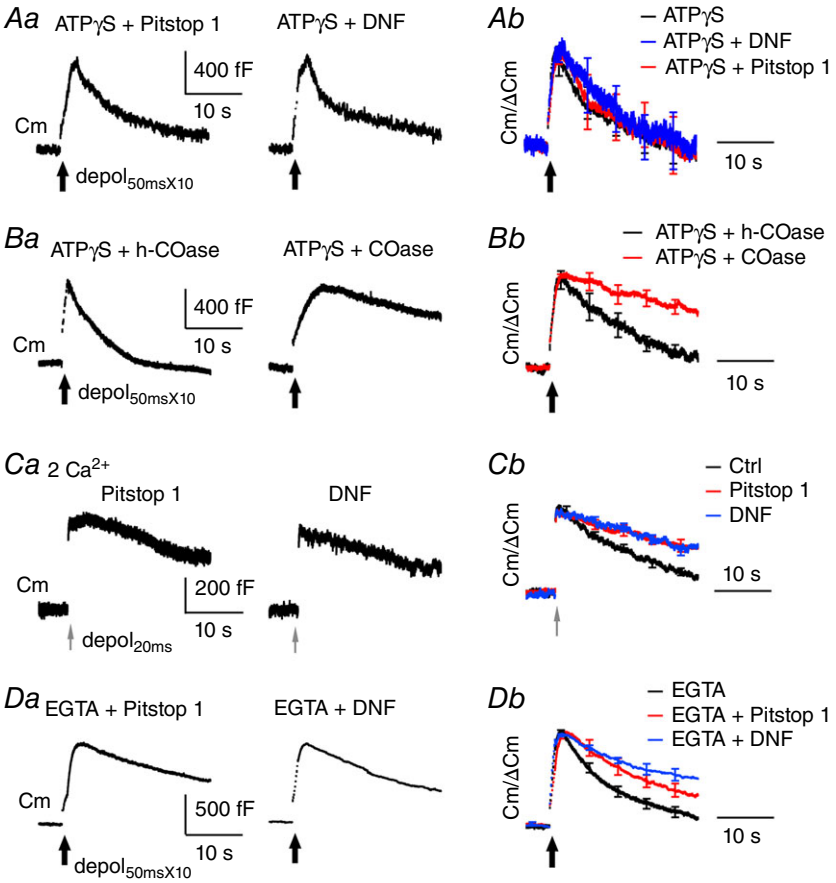

Figure 4. ATP-independent endocytosis involves cholesterol but not acute maturation of clathrin-coat
A and *B*, sampled Cm responses to $depol_{50msX10}$ recorded from calyces co-dialysed with 4 mM ATPγS and one of the following chemicals: 80 μM Pitstop 1 ($n = 10$), 100 μM DNF ($n = 7$), 10 U ml^{-1} heat-inactivated COase (h-COase, $n = 6$) and 10 U ml^{-1} COase ($n = 7$). Average Cm traces after normalization to ΔCm are superimposed (right) to compare endocytosis kinetics. *C*, sampled and average Cm responses induced by $depol_{20ms}$ from calyces dialysed with 80 μM Pitstop 1 ($n = 6$) or 100 μM DNF ($n = 8$). Average Cm traces after normalization to ΔCm are superimposed (right) to compare endocytosis kinetics with control (Fig. 2*A*). *D*, sampled and average Cm responses upon $depol_{50msX10}$ from calyces dialysed with 20 mM EGTA along with 80 μM Pitstop 1 ($n = 6$) or 100 μM DNF ($n = 10$). Compared to EGTA alone (trace from Fig. 3*D*), such co-dialysis with Pitstop 1 or DNF induced additional inhibition of endocytosis. Bath Ca^{2+} was 6 mM except for 2 mM in (*C*).

over 25 s after $depol_{50msX10}$, or ~10% of the membrane expansion from exocytosis (599 ± 56 fF). The effects of EGTA and ATPγS are much stronger than those of EGTA or ATPγS (Fig. 1*E* and *F*) alone, indicating that EGTA and ATPγS preferentially target different components in excess endocytosis. EGTA blocked endocytosis resistant to ATPγS, as well as endocytosis of pre-existing membrane, suggesting that ATP-independent endocytosis retrieves pre-existing membrane.

Second, we attempted isolating endocytosis of pre-existing membrane by minimizing newly fused membrane with the light chain of botulinum toxin C (T/C). T/C can cleave syntaxin and prevent vesicles from priming and fusion (Blasi *et al.* 1993). At ~7 min after dialysis, T/C (0.5 μM) reduced exocytosis following $depol_{50msX10}$ ($\Delta Cm = 631 \pm 50$ fF, $n = 8$, $P < 0.01$) (Fig. 3*E*) but did not significantly change $Rate_{endo}$ (295 ± 60 fF s^{-1}, $P = 0.12$) or the amount of endocytosis overshoot ($Endo_{25s} = 1283 \pm 272$ fF, overshoot $\Delta Cm\text{-}Endo_{25s} = -652 \pm 258$ fF, $P = 0.75$ *vs.* -741 ± 90 fF in control). The overshoot was observed even in one calyx where exocytosis was absent (not shown). T/X highlighted endocytosis of pre-existing membrane by reducing exocytosis. Interestingly, co-dialysis with EGTA and T/C caused stronger inhibition of endocytosis ($Rate_{endo} = 36 \pm 10$ fF s^{-1} and $Endo_{25s} = 417 \pm 173$ fF, $n = 5$) than EGTA or T/C alone ($P < 0.01$) (Fig. 3*E*), suggesting that endocytosis of pre-existing membrane is blocked by EGTA but not T/C. On the other hand, co-dialysis with ATPγS and T/C reduced $Rate_{endo}$ to 105 ± 37 fF s^{-1} ($n = 8$) and $Endo_{25s}$ to 609 ± 160 fF, which is similar to ATPγS alone ($P = 0.41$ and 0.24, respectively). This effect indicates that T/C does not affect ATP-independent endocytosis.

In summary, ATP-independent endocytosis mainly retrieved pre-existing membrane, which could be blocked by EGTA but not T/C, whereas ATP-dependent endocytosis mainly retrieved newly fused membrane, which was less sensitive to EGTA. Because ATP-dependence of synaptic endocytosis has been well recognized, we next focused on the mechanisms and importance of ATP-independent endocytosis at calyces.

ATP-independent endocytosis does not involve clathrin-coat maturation

A previous study suggests that endocytosis of pre-existing membrane is similar to slow compensatory endocytosis in requiring GTP, dynamin, calmodulin and calcineurin (Xue *et al.* 2012). In the present study, we tested whether

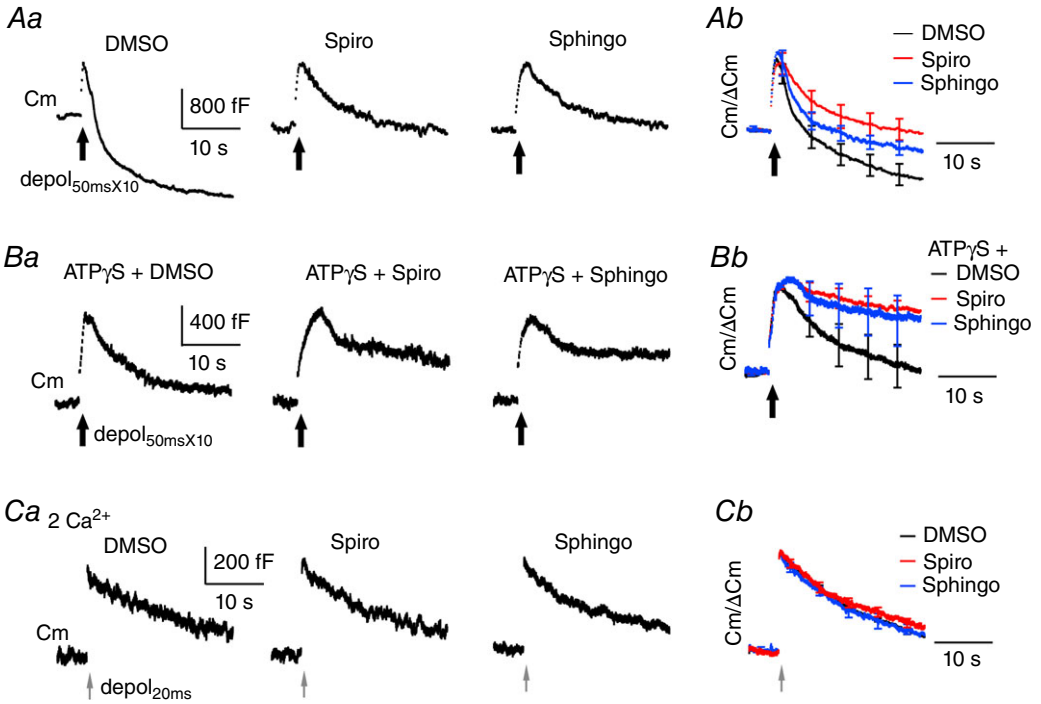

Figure 5. Inhibitors of nSMase impair ATP-independent endocytosis
A and *B*, sampled (left) and average (right) Cm responses to $depol_{50msX10}$ under dialysis with DMSO (0.1%, $n = 12$), 10 μM spiroepoxide (Spiro, $n = 12$), 30 μM sphingolactone-24 (Sphingo, $n = 9$), 4 mM ATPγS with DMSO ($n = 11$), ATPγS with spiroepoxide ($n = 10$) or ATPγS with sphingolactone-24 ($n = 11$). Bath Ca^{2+} was 6 mM. *C*, sampled Cm (left) and average (right) responses to $depol_{20ms}$ under dialysis with DMSO ($n = 9$), spiroepoxide ($n = 11$) or sphingolactone-24 ($n = 11$). Bath Ca^{2+} was 2 mM.

ATP-independent endocytosis and compensatory endocytosis similarly require clathrin by examining effects of blocking clathrin-coated pit maturation. When calyces were dialysed with ATPγS and Pitstop 1 (80 μM), a small molecule inhibitor of clathrin-coated pit maturation (von Kleist *et al.* 2011), endocytosis following depol$_{50msX10}$ started at 149 ± 30 fF s^{-1} (n = 10) and retrieved membrane of 804 ± 146 fF within 25 s (Fig. 4*A*). These measurements are similar to those for ATPγS alone. Similarly, co-dialysis with ATPγS and DNF (100 μM, n = 7), a 12-mer peptide that inhibits formation of clathrin-coated pits by disrupting interaction between amphiphysin and the AP2 adaptor complex (Jockusch *et al.* 2005; Hosoi *et al.* 2009; Wu *et al.* 2009; Yue & Xu, 2015), did not inhibit endocytosis more than ATPγS (Fig. 4*A* and Table 1).

By contrast to failure of Pitstop 1 and DNF, ATP-independent endocytosis was sensitive to COase (10 U ml^{-1}), which has been widely used to reduce membrane cholesterol by oxidization of cholesterol into 4-cholesten-3-one (Assaife-Lopes *et al.* 2010; Mercer *et al.* 2012; Korinek *et al.* 2015). Co-dialysis with COase and ATPγS caused stronger inhibition of endocytosis (Rate$_{endo}$ = 58 ± 17 fF s^{-1}, P = 0.12 and Endo$_{25s}$ = 334 ± 57 fF, P < 0.01, n = 7) than ATPγS (Fig. 4*B*). As a control, COase was first inactivated in boiling water for 10 min (Torabi *et al.* 2007) and co-dialysed with ATPγS into calyces. The heat-inactivated COase did not further inhibit endocytosis in the presence of ATPγS. These data collectively suggest that ATP-independent endocytosis requires cholesterol but not acute maturation of clathrin-coated pits.

By contrast to ATP-independent endocytosis, the slow endocytosis following depol$_{20ms}$ was significantly impaired by Pitstop 1 or DNF (Fig. 4*C* and Table 1), which is consistent with our previous observations (Wu *et al.* 2009; Yue & Xu, 2015). Accordingly, does excess endocytosis following depol$_{50msX10}$ involve clathrin at all? Because EGTA (20 mM) preferentially blocked ATP-independent endocytosis following depol$_{50msX10}$ (Fig. 3*C*–*E*), we examined EGTA-resistant endocytosis at calyces dialysed with EGTA and Pitstop 1 (n = 6) or EGTA and DNF (n = 10) (Fig. 4*D*). Compared to EGTA, co-dialysis of EGTA and Pitstop 1 resulted in slower Rate_endo (83 ± 25 fF s^{-1} *vs.* 159 ± 18 fF s^{-1} for EGTA, P < 0.05) (Table 1) and less membrane retrieval at 25 s after depol$_{50msX10}$ (843 ± 155 fF *vs.* 1201 ± 87 fF for EGTA, P = 0.16), indicating inhibition of EGTA-resistant endocytosis by Pitstop 1. Co-dialysis of EGTA and DNF caused similar effects. To summarize, we suggest that acute maturation of clathrin-coated pits is involved in ATP-dependent endocytosis following either depol$_{20ms}$ or depol$_{50msX10}$ but not in ATP-independent endocytosis.

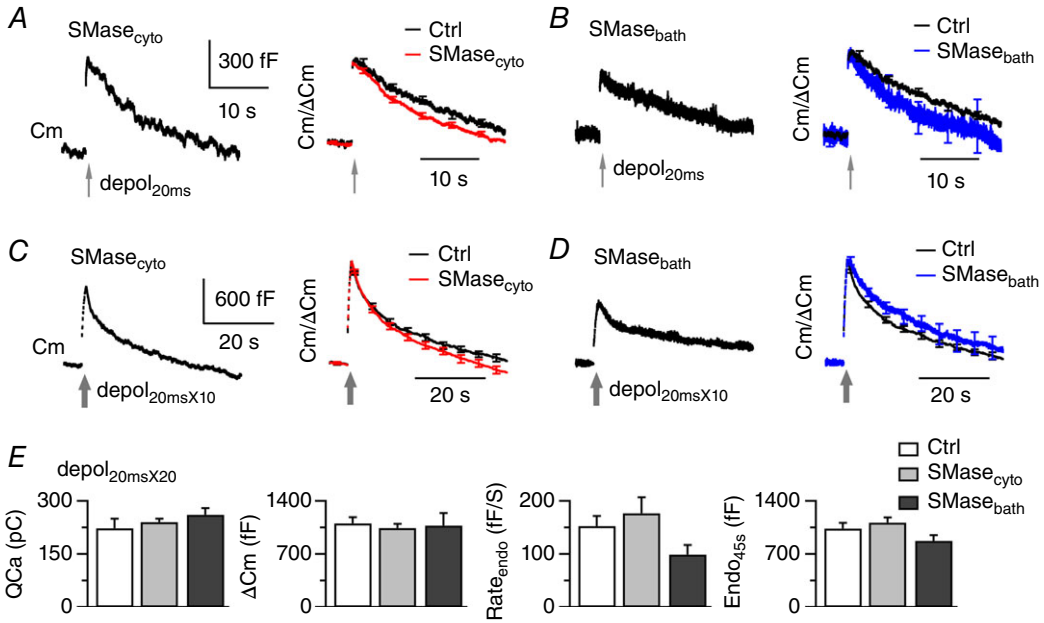

Figure 6. Exogenous SMase does not significantly affect compensatory endocytosis
A, sampled Cm responses to depol$_{20ms}$ under dialysis with SMase (SMase$_{cyto}$: 1 U ml^{-1}, left). Right: superimposed Cm traces after normalization to ΔCm (n = 12 for SMase$_{cyto}$). Control (n = 7) is from Fig. 2*A*. Bath Ca^{2+} was 2 mM. *B*, similar to (*A*), except that this calyx was exposed to SMase in the bath for > 30 min (1 U ml^{-1}, left). Average results are from six calyces exposed to bath SMase. *C* and *D*, similar to the description in (*A*) to (*B*) except that calyces were stimulated with depol$_{20msX10}$. *E*, comparison of QCa, ΔCm, Rate$_{endo}$ and Endo$_{45s}$ for control (n = 10 from Fig. 1*C*), SMase$_{cyto}$ (n = 11) and SMase$_{bath}$ (n = 9). [Colour figure can be viewed at wileyonlinelibrary.com]

Sphingomyelinase regulates ATP-independent endocytosis

Cholesterol involvement in ATP-independent endocytosis led our attention to SMase, which is found in cholesterol-enriched membranes at high levels. Application of exogenous SMase can induce ATP-independent endocytosis of large vesicles at macrophages, fibroblasts (Zha *et al.* 1998) and baby hamster kidney cells (Lariccia *et al.* 2011). Because reducing cholesterol by intracellular dialysis of COase (Fig. 4) and cyclodextrin (Yue & Xu, 2015) inhibited ATP-independent endocytosis or endocytosis of pre-existing membrane, we hypothesized that ATP-independent endocytosis is modulated by neutral SMase (nSMase) (Liu *et al.* 1998), the dominant

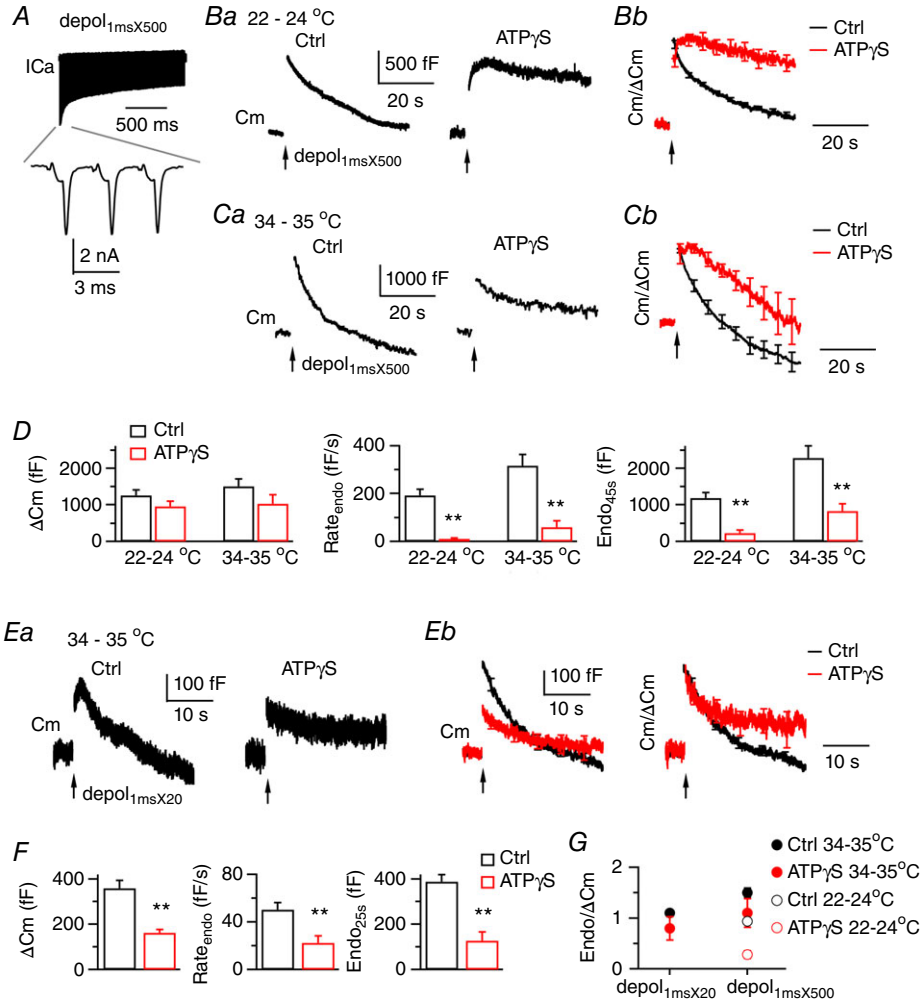

Figure 7. Temperature promotes ATP-independent endocytosis
A, ICa currents induced by $depol_{1msX500}$ from a control calyx, which was perfused by 22–24°C solution containing 2 mM Ca^{2+}. The lower trace shows ICa induced by the first three pulses. *B* and *C*, sampled Cm responses (*Ba* and *Ca*) to $depol_{1msX500}$ under dialysis with control or 4 mM ATPγS. Calyces were perfused by bath solution of 22–24°C or 34–35°C. Average Cm traces after normalization to ΔCm are superimposed in (*Bb*) and (*Cb*). At calyces dialysed with ATPγS, $depol_{1msX500}$ triggered a more significant amount of endocytosis at 34–35°C, which largely reset membrane expansion from exocytosis. *D*, ΔCm, $Rate_{endo}$ and $Endo_{45s}$ induced by $depol_{1msX500}$ from control (n = 10) and ATPγS (n = 9) at 22–24°C, as well as control (n = 9) and ATPγS (n = 9) at 34–35°C. *E*, sampled Cm responses (*Ea*) induced by $depol_{1msX20}$ from calyces perfused by solution of 34–35°C. The example for ATPγS represents intermediate inhibition of endocytosis. In some examples that are not shown, endocytosis was either almost fully blocked, or induced endocytosis overshoot. Average Cm traces without (*Eb*, left, 11 calyces for control, 10 calyces for ATPγS) and with normalization to ΔCm (*Eb*, right) are superimposed. $Depol_{1msX20}$ triggered a significant component of ATP-independent endocytosis. *F*, ΔCm, $Rate_{endo}$ and $Endo_{45s}$ induced by $depol_{1msX20}$ from control (n = 11) and ATPγS (n = 10) at 34–35°C. *G*, $Endo_{45s}$ ($depol_{1msX500}$) or $Endo_{25s}$ ($depol_{1msX20}$) normalized to ΔCm. At 34–35°C, $depol_{1msX500}$ and $depol_{1msX20}$ induced significant ATP-independent endocytosis to recover membrane close to the amount of exocytosis, resulting in a value near 1 for Endo/ΔCm. [Colour figure can be viewed at wileyonlinelibrary.com]

SMase on cytosolic leaflet of plasma membrane. To test this hypothesis, we examined effects of two selective nSMase inhibitors, spiroepoxide (Arenz & Giannis, 2000; Trajkovic *et al.* 2008) and sphingolactone-24 (Wascholowski & Giannis, 2006; Lin *et al.* 2011).

Dialysis with 10 μM spiroepoxide, or 30 μM sphingolactone 24, led to partial inhibition of excess endocytosis induced by $depol_{50msX10}$ (Fig. 5*A* and Table 1). For example, spiroepoxide reduced $Rate_{endo}$ to 285 ± 48 fF s^{-1} (n = 12, P = 0.05 *vs.* 455 ± 38 fF s^{-1} in 0.1% DMSO, n = 12) and $Endo_{25s}$ to 1347 ± 147 fF (P < 0.05 *vs.* 1888 ± 153 fF in DMSO). This inhibition was on ATP-independent endocytosis, as suggested by the evidence reported below.

First, spiroepoxide or sphingolactone 24 reduced the remaining endocytosis in the presence of ATPγS. Compared to co-dialysis with ATPγS and DMSO, co-dialysis with ATPγS and spiroepoxide (10 μM) did not affect exocytosis following $depol_{50msX10}$ (Fig. 5*B* and Table 1) but decreased $Rate_{endo}$ from 149 ± 24 fF s^{-1} (n = 9) to 63 ± 25 fF s^{-1} (n = 10, P < 0.05) and membrane recovery from 908 ± 135 fF to 341 ± 55 fF (P < 0.01). Co-dialysis with ATPγS and sphingolactone-24 (30 μM) produced similar effects. Second, spiroepoxide

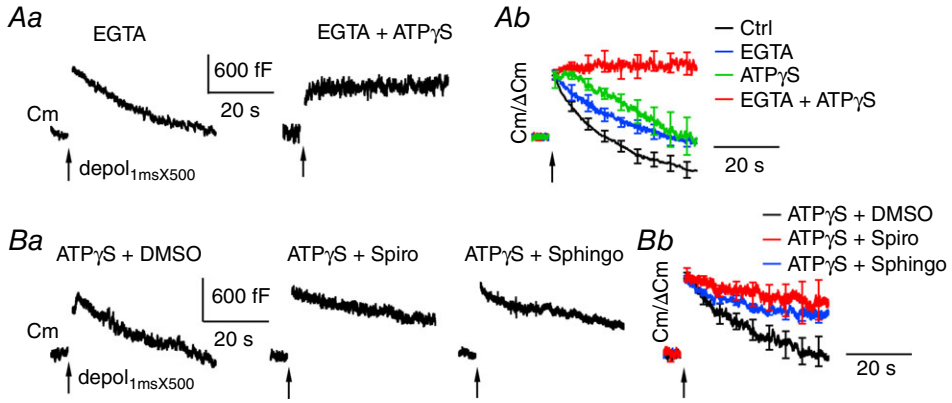

Figure 8. EGTA and inhibitors of nSMase impair ATP-independent endocytosis at near physiological temperature
A, sampled Cm responses (*Aa*) to $depol_{1msX500}$ from calyces dialysed with 10 mM EGTA, or ATPγS and EGTA, at 34–35°C. *Ab*, average Cm traces after normalization to ΔCm are from control (n = 12), EGTA (n = 8), ATPγS (n = 8) and ATPγS and EGTA (n = 8). *B*, sampled Cm responses (*Ba*) to $depol_{1msX500}$ under dialysis with ATPγS and DMSO (0.1%), ATPγS and 10 μM spiroepoxide, or ATPγS and 30 μM sphingolactone-24 at 34–35°C. *Bb*, average Cm traces after normalization to ΔCm are from ATPγS and DMSO (n = 8), ATPγS and spiroepoxide (n = 9) and ATPγS and sphingolactone-24 (n = 9).

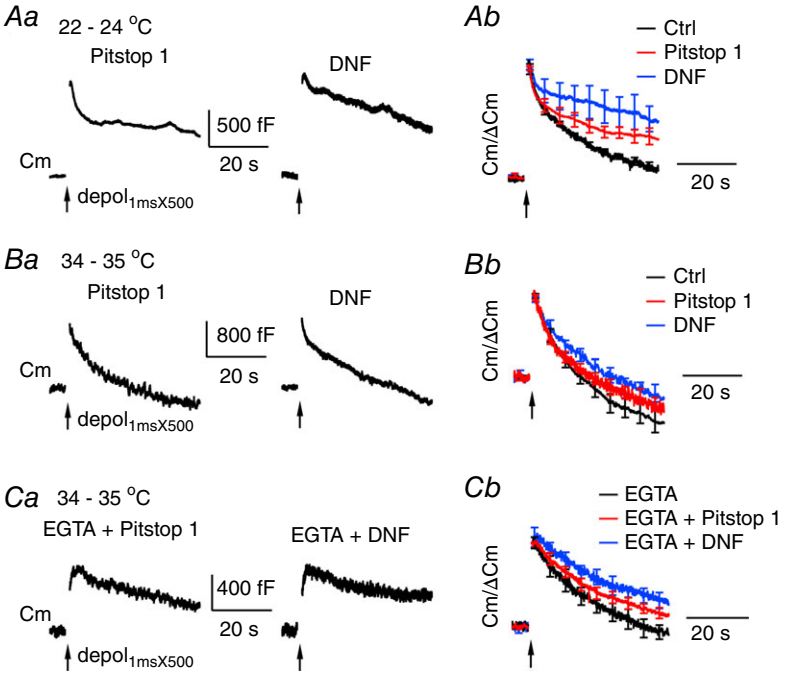

Figure 9. Clathrin-mediated endocytosis has a minor contribution to endocytosis at near physiological temperature
A, sampled Cm responses (*Aa*) to $depol_{1msX500}$ from calyces dialysed with 80 μM Pitstop 1 or 100 μM DNF at 22–24°C. *Ab*, average Cm traces after normalization to ΔCm are superimposed for control (Fig. 7), Pitstop 1 (n = 11) and DNF (n = 7). *B*, same as in (*A*), except that data are from tests performed at 34–35°C. *Bb*, superimposed traces are for control (Fig. 7), Pitstop 1 (n = 6) and DNF (n = 8). *C*, sampled Cm responses (*Ca*) to $depol_{1msX500}$ under dialysis with 10 mM EGTA and 80 μM Pitstop 1, or EGTA and 100 μM DNF, at 34–35°C. *Cb*, average Cm traces after normalization to ΔCm are superimposed for EGTA (Fig. 7*A* and *B*), EGTA and Pitstop 1 (n = 6) and EGTA and DNF (n = 7).

Table 1. QCa and changes of Cm induced by depolarization at 22–24°C

Stimulation	Treatment	QCa (pC)	ΔCm (fF)	Rate_endo (fF s^{-1})	$Endo_{25s}$ (fF)
$Depol_{50msX10}$	Ctrl	614 ± 33	1199 ± 80	430 ± 41	1939 ± 125
	ATPγS	637 ± 55	784 ± 99	141 ± 25	796 ± 69
	AMP-PNP	570 ± 44	735 ± 91	219 ± 63	935 ± 169
	EGTA	884 ± 48	1348 ± 74	183 ± 27	1201 ± 87
	ATPγS + EGTA	785 ± 36	599 ± 56	10 ± 3	59 ± 15
	T/C	808 ± 87	631 ± 50	295 ± 60	1283 ± 272
	EGTA + T/C	779 ± 49	839 ± 198	36 ± 10	417 ± 173
	ATPγS + T/C	560 ± 68	805 ± 135	105 ± 37	609 ± 160
	ATPγS + Pitstop 1	627 ± 44	855 ± 78	149 ± 30	804 ± 146
	ATPγS + DNF	687 ± 98	804 ± 112	132 ± 33	924 ± 297
	ATPγS + h-COase	612 ± 27	843 ± 73	144 ± 43	718 ± 56
	ATPγS + COase	621 ± 29	869 ± 105	58 ± 17	334 ± 57
	EGTA + pitstop1	884 ± 77	1270 ± 186	83 ± 25	843 ± 155
	EGTA + DNF	813 ± 53	883 ± 81	42 ± 4	507 ± 91
	T/C + Pitstop1	605 ± 39	431 ± 47	195 ± 45	968 ± 178
	DMSO	630 ± 26	1107 ± 104	455 ± 38	1888 ± 153
	Spiro	643 ± 26	1121 ± 89	285 ± 48	1347 ± 147
	Spingo	647 ± 44	1118 ± 83	319 ± 46	1386 ± 128
	ATPγS + DMSO	729 ± 67	1013 ± 110	149 ± 24	908 ± 135
	ATPγS + Spiro	662 ± 40	1076 ± 96	63 ± 25	341 ± 55
	ATPγS + Sphingo	734 ± 38	792 ± 111	69 ± 17	343 ± 86
$Depol_{20ms}$	Ctrl	34 ± 3	443 ± 20	30 ± 3	378 ± 19
	ATPγS	36 ± 2	307 ± 33	3 ± 2	25 ± 12
	AMP-PNP	36 ± 2	320 ± 24	4 ± 1	20 ± 10
	0 mM GTP	28 ± 4	385 ± 33	9 ± 4	69 ± 37
	3 mM GTP	34 ± 2	371 ± 45	27 ± 5	324 ± 36
	ATPγS + 3 mM GTP	34 ± 3	210 ± 48	2 ± 1	9 ± 8
	Pitstop 1	31 ± 1	424 ± 33	15 ± 3	176 ± 32
	DNF	37 ± 1	412 ± 36	8 ± 2	198 ± 29
	DMSO	38 ± 2	402 ± 33	29 ± 4	339 ± 35
	Spiro	34 ± 2	378 ± 24	22 ± 3	278 ± 24
	Sphingo	39 ± 3	423 ± 25	29 ± 3	363 ± 33
	$SMase_{cyto}$	33 ± 1	433 ± 11	38 ± 13	417 ± 22
	$SMase_{bath}$	34 ± 2	370 ± 57	34 ± 2	353 ± 37

or sphingolactone 24 did not affect endocytosis induced by $depol_{20ms}$ at calyces in 2 mM bath Ca^{2+} (Fig. 5*C*). This endocytosis was instead blocked by ATPγS or AMP-PNP (Fig. 1*B* and *C*). Therefore, inhibition of nSMase impaired excess endocytosis by targeting ATP-independent endocytosis. Our results suggest that the activity of nSMase on the cytosolic membrane leaflet modulates ATP-independent endocytosis of pre-existing membrane.

We further examined whether exogenous SMase promotes endocytosis as in non-neuronal cells (Rosa *et al.* 2010; Lariccia *et al.* 2011). Dialysis with bacterial SMase (1 U ml^{-1}) for > 5 min, or bath incubation with SMase for 15–75 min, slightly facilitated slow compensatory endocytosis following $depol_{20ms}$ (Fig. 6*A* and *B* and Table 1) but caused no significant effects on endocytosis following $depol_{20msX10}$ (Fig. 6*C*–*E*). Therefore, globally increasing intra- or extracellular SMase by exogenous supply failed to drastically facilitate endocytosis as in non-neuronal cells (Rosa *et al.* 2010; Lariccia *et al.* 2011). These results suggest that modulation of endocytosis by endogenous SMase depends on membrane domains. We thus did not further test the effects of supplying exogenous sphingolipids.

Temperature recruits ATP-independent endocytosis of pre-existing membrane

In the experiments described above, we induced endocytosis by prolonged depolarization pulse(s) at room temperature. We were also interested in how ATP-independent endocytosis contributes under more physiological conditions. The calyx of Held is a synapse responsible for sound localization, and can relay neuronal information with high fidelity even at firing rates of several hundred Hz (von Gersdorff & Borst,

Table 2. Changes of Cm induced by $Depol_{1msX500}$

Temperature	Treatment	ΔCm (fF)	Rate_endo (fF s^{-1})	$Endo_{45s}$ (fF)
22–24°C	Ctrl	1255 ± 153	192 ± 26	1180 ± 153
	ATPγS	950 ± 146	11 ± 4	230 ± 82
	Pitstop 1	1313 ± 176	224 ± 44	767 ± 110
	DNF	1469 ± 100	188 ± 45	758 ± 157
34–35°C	Ctrl	1502 ± 204	317 ± 47	2284 ± 334
	ATPγS	1022 ± 248	60 ± 26	825 ± 201
	EGTA	738 ± 124	70 ± 11	756 ± 148
	ATPγS + EGTA	544 ± 88	5 ± 3	56 ± 43
	ATPγS + DMSO	912 ± 170	57 ± 13	764 ± 140
	ATPγS + Spiro	727 ± 136	26 ± 14	227 ± 75
	ATPγS + Sphingo	881 ± 105	50 ± 13	447 ± 65
	Pitstop 1	1320 ± 153	210 ± 46	1797 ± 232
	DNF	1286 ± 107	192 ± 34	1622 ± 105
	EGTA + Pitstop 1	860 ± 77	55 ± 11	743 ± 78
	EGTA + DNF	664 ± 60	35 ± 7	494 ± 63

2002). Therefore, we evaluated the contribution of the ATP-independent mechanism at an experimental temperature of 34–35°C, applying stimulation with 500 pulses of 1 ms depolarization from −80 mV to 0 mV at 333 Hz (referred to as $depol_{1msX500}$) or 20 such pulses at 100 Hz (referred to as $depol_{1msX20}$). The brief pulse mimics an action potential in triggering a similar amount of neurotransmitter release and is preferred for convenience with respect to protocol design (Xu & Wu, 2005). We recorded the Ca^{2+} channel current (Fig. 7*A*) but did not quantify it because accurate measurement of leak channel current was difficult for later brief pulses.

At calyces perfused with bath solution of 34–35°C, $depol_{1msX500}$ evoked exocytosis of 1502 ± 204 fF (n = 12) (Table 2), followed by fast endocytosis ($Rate_{endo}$ = 317 ± 47 fF s^{-1}) with an overshoot of 731 ± 114 fF (Fig. 7*C*). Dialysis with ATPγS led to partial inhibition of endocytosis ($Rate_{endo}$ = 60 ± 26 fF s^{-1}, n = 8), which recovered membrane by 825 ± 201 fF within 45 s after $depol_{1msX500}$, or 80.7% of membrane expansion from exocytosis (ΔCm = 1022 ± 248 fF). By contrast, at 22–24°C, endocytosis following $depol_{1msX500}$ was initially 192 ± 26 fF s^{-1} (n = 9) and had no significant overshoot at control (ΔCm = 1255 ± 153 fF and $Endo_{45s}$ = 1180 ± 153 fF). ATPγS largely abolished this endocytosis ($Rate_{endo}$ = 11 ± 4 fF s^{-1} and $Endo_{45s}$ = 230 ± 82 fF, n = 8). These results suggest that temperature recruits ATP-independent endocytosis. Stimulation with the milder $depol_{1msX20}$ similarly recruited ATP-independent endocytosis, which had a rate of 23 ± 6 fF s^{-1} (n = 10, P < 0.01 *vs.* 50 ± 6 fF s^{-1} in the presence of ATP, n = 11) (Fig. 7*E* and *F*). Based on Cm recordings from hippocampal and cerebellar mossy fibre synapses under 36°C, a single action potential waveform induces ultrafast Cm decay (τ = ∼470 ms), which represents a form of clathrin independent, actin-dependent endocytosis (Delvendahl *et al.* 2016). We are unable to investigate this possible mechanism at calyces because the noise in our whole-cell recordings was too large for us to identify a small, ultrafast Cm transient.

To test whether the regulatory mechanisms underlying ATP-independent endocytosis change with elevated temperature, we studied the effects of EGTA and nSMase inhibitors on endocytosis induced by $depol_{1msX500}$ at 34–35°C (Fig. 8 and Table 2). EGTA (10 mM) partially inhibited endocytosis following $depol_{1msX500}$ ($Rate_{endo}$ = 70 ± 11 fF s^{-1} and $Endo_{45s}$ = 756 ± 148 fF, n = 8) (Fig. 8*A*). However, co-dialysis with ATPγS and EGTA caused a strikingly full block of endocytosis, and restricted membrane retrieval to 56 ± 43 fF (n = 8) or ∼10% of the surface expansion as a result of exocytosis (ΔCm = 544 ± 88 fF). Furthermore, co-dialysis with ATPγS and spiroepoxide (10 μM), or ATPγS and sphingolactone 24 (30 μM), caused more severe inhibition on membrane retrieval than ATPγS (P < 0.05 for both co-dialysis) (Fig. 8*B*). These results are similar to those obtained at room temperature, suggesting that temperature does not change the regulatory mechanisms of ATP-independent endocytosis.

Clathrin-mediated endocytosis plays a minor role at elevated temperature

At room temperature, clathrin-mediated endocytosis is a dominant mechanism of slow endocytosis at the calyx of Held (Hosoi *et al.* 2009; Wu *et al.* 2009; Yue & Xu, 2015), whereas ATP-independent endocytosis only had a small contribution (Fig. 1*A*). To compare the contributions of both mechanisms at elevated temperature, we tested the

inhibitors DNF and Pitstop 1 on endocytosis induced by $depol_{1msX500}$ (Fig. 9 and Table 2). At 22–24°C, Pitstop 1 or DNF strikingly inhibited slow endocytosis following $depol_{1msX500}$ without significantly affecting the initial rapid endocytosis (Fig. 9*A*), which is similar to effects of DNF at retina bipolar cells (Jockusch *et al.* 2005). Compared to control (Fig. 7*A*), Pitstop 1 and DNF reduced membrane retrieval from 1180 ± 153 fF to 767 ± 110 fF ($n = 11$) and 758 ± 157 fF ($n = 7$), respectively. These amounts of membrane retrieval correspond to 93 ± 2% of ΔCm in control, 62 ± 7% in Pitstop 1 ($P < 0.05$) and 50 ± 9% in DNF ($P < 0.01$), respectively, which indicates severely impaired efficiency in recovering the exocytosed membrane. At 34–35°C, the membrane retrieval was 152 ± 7% of ΔCm in control, 138 ± 6% in Pitstop 1 ($P = 0.1$, $n = 6$) and 120 ± 7% in DNF ($P < 0.05$, $n = 8$), respectively (Fig. 9*B*). Less reduction of endocytosis efficiency by DNF and Pitstop 1 implies a smaller contribution from clathrin-mediated endocytosis at elevated temperature. To avoid an underestimate as a result of interference from ATP-independent endocytosis, we further tested co-dialysis with the inhibitors and 10 mM EGTA. Compared to EGTA alone ($n = 8$) (Fig. 9*C*), co-dialysis with DNF and EGTA decreased $Rate_{endo}$ following $depol_{1msX500}$ from 70 ± 11 fF s^{-1} to 35 ± 7 fF s^{-1} ($n = 7$, $P < 0.05$) and slightly reduced membrane retrieval ($Endo_{45s}$) from 756 ± 148 fF to 494 ± 68 fF. Co-dialysis with Pitstop1 and EGTA showed a similar trend but insignificant effects ($Rate_{endo}$ = 54 ± 9 fF s^{-1} and $Endo_{45s}$ = 743 ± 78 fF, $n = 6$). The membrane retrieval was 100 ± 6% of ΔCm in EGTA, 85 ± 5% in Pitstop 1 and EGTA ($P < 0.05$, $n = 7$) and 70 ± 3% in DNF and EGTA ($P < 0.05$, $n = 7$), respectively (Fig. 9*C*). In summary, Pitstop 1 and DNF blocked a smaller fraction of endocytosis evoked by $depol_{1msX500}$ at 34–35°C, suggesting a minor contribution of clathrin-mediated endocytosis at elevated temperature, which is consistent with recent studies (Watanabe *et al.* 2013, 2014; Delvendahl *et al.* 2016).

Discussion

The novel findings of the present study are that recruitment of ATP-independent endocytosis is a major cause of activity- and temperature-dependent acceleration of endocytosis at calyx-type central nerve terminals, and also that ATP-independent endocytosis primarily retrieves pre-existing membrane by a non-canonical, lipid-regulated mechanism.

Both rapid and slow forms of compensatory endocytosis require ATP

Most studies suggest that endocytosis at nerve terminals requires ATP. Blocking ATP hydrolysis impairs compensatory endocytosis at synapses such as retina bipolar cells (Heidelberger, 2001), rod photoreceptors of salamander retina (Van Hook & Thoreson, 2012) and hippocampal boutons (Rangaraju *et al.* 2014; Pathak *et al.* 2015). One exception is the cone photoreceptors of salamander retina where endocytosis is very rapid (τ = 250 ms) and ATP-independent (Van Hook & Thoreson, 2012). In the present study, blocking ATP hydrolysis with ATPγS or AMP-PNP largely eliminated slow (τ = 14.9–19.4 s) and rapid forms (τ = 1.8 s) of compensatory endocytosis at calyces (Figs 1, 2 and 7*B*). Slow endocytosis has been shown to depend on GTP, dynamin and clathrin (Yamashita *et al.* 2005; Xu *et al.* 2008; Hosoi *et al.* 2009; Wu *et al.* 2009), whereas rapid endocytosis following $depol_{20msX10}$ depends on GTP hydrolysis and probably also dynamin (Xu *et al.* 2008), although not clathrin based on the results from other synapses (Jockusch *et al.* 2005). The similar sensitivity to ATPγS and AMP-PNP (Figs 1 and 2) implies that slow endocytosis and rapid endocytosis at calyces share most, if not all, of the ATP-dependent steps leading to membrane retrieval. Indeed, both mechanisms can involve calmodulin (Wu *et al.* 2009; Yamashita *et al.* 2010; Yao & Sakaba, 2012), calcineurin (Wu *et al.* 2009; Yamashita *et al.* 2010; Yao & Sakaba, 2012), myosin light chain kinase/myosin (Yue & Xu, 2014) and actin polymerization (Wu *et al.* 2016), which rely on ATP hydrolysis for functions. Individual blocking of these molecules inhibits endocytosis to a lesser extent than ATPγS or AMP-PNP, implying that their collective needs for ATP contribute to an absolute ATP requirement in rapid and slow endocytosis. By contrast to an early study at *Drosophila* synapses (Krishnan *et al.* 2001), our experiments do not support that endocytosis depends on acute regeneration of GTP using ATP (Fig. 2*D* and *E*). Whether rapid endocytosis and slow endocytosis involve other unidentified ATP-dependent processes, such as disassembly of soluble *N*-ethylmaleimide-sensitive factor attachment protein receptor complexes, remains to be determined. Regardless of activity and temperature, endocytosis at calyces always contained a contribution from ATP-dependent mechanisms, although with variable fraction. By demonstrating similar ATP-dependence in rapid and slow endocytosis, the present study has extended beyond current reports of ATP-dependent endocytosis (Heidelberger, 2001; Rangaraju *et al.* 2014; Pathak *et al.* 2015).

Activity and temperature recruit ATP-independent endocytosis

Interestingly, calyces also retrieved membrane via an ATP-independent mechanism. Inhibition of endocytosis by ATPγS or AMP-PNP became less complete following intense stimulation (Figs 1 and 2) and at elevated temperature (Fig. 7). At calyces dialysed with ATPγS

or AMP-PNP at 22–24°C (Figs 1 and 2), $Rate_{endo}$ of the remaining endocytosis was 3 or 4 fF s^{-1} after $depol_{20ms}$, or 8–10% of endocytosis in control (30 fF s^{-1}), but increased to 141 or 219 fF s^{-1} after $depol_{50msX10}$, or 30–50% of endocytosis in control (430 fF s^{-1}). Contribution of ATP-independent mechanisms to endocytosis kinetics increased by ∼4-fold from 8–10% to 30–50%. Elevating temperature to 34–35°C also caused an ∼4 fold increase of the contribution of ATP-independent endocytosis following $depol_{1msX500}$ (Fig. 7*B* and *C*). The temperature-dependent facilitation may result from multiple factors, including enhancement of Ca^{2+} channel current (Renden & von Gersdorff, 2007) and/or alteration of physical status of membrane sphingomyelin/cholesterol (de Almeida *et al.* 2003). Therefore, recruitment of ATP-independent endocytosis is a major mechanism underlying endocytosis acceleration at intense activity and physiological temperature. Another non-canonical, GTP-independent component of endocytosis has been observed previously at young calyces (Xu *et al.* 2008) but disappears at calyces of P13–14 (Yamashita *et al.* 2010). By contrast, $depol_{50msX10}$ induced ATP-independent endocytosis at calyces from both P8–11 (Fig. 1*E* and *F*) and P14–15 rats (Fig. 2*F*–*H*). The ATP-independent amount at post-hearing calyces appeared smaller, probably because maturation of synapses leads to more confined Ca^{2+} domains and initiation of endocytosis at closer locations around open Ca^{2+} channels. Its contribution, however, was significant and equivalent to 80% of the exocytosed membrane. Therefore, ATP-independent endocytosis continues to play an important role and function along with ATP-dependent endocytosis at post-hearing calyces.

Previous studies have reported that activation of bulk endocytosis and ultrafast endocytosis underlies the acceleration of endocytosis under intense activity (Cheung & Cousin, 2013; Kokotos & Cousin, 2015) and elevated temperature (Watanabe *et al.* 2013, 2014), respectively. Both mechanisms retrieve efficiently from the plasma membrane to form endosomes, which are subsequently processed to generate synaptic vesicles (Cheung & Cousin, 2013; Watanabe *et al.* 2014; Kokotos & Cousin, 2015). Because endosomes are multiple times larger than vesicles, an interesting question is whether, similar to ATP-independent endocytosis, these mechanisms contribute to produce excess endocytosis at nerve terminals. On the other hand, bulk endocytosis and ultrafast endocytosis rely on actin polymerization that depends on ATP (Holt *et al.* 2003; Nguyen *et al.* 2012; Watanabe *et al.* 2013), whereas the mechanism that we suggest did not require ATP or actin polymerization (Yue & Xu, 2015). Furthermore, ultrafast endocytosis completes within 100 ms (Watanabe *et al.* 2013, 2014), whereas ATP-independent endocytosis had normal time constants of seconds to tens of seconds. In addition, unlike slow compensatory endocytosis (Hosoi *et al.* 2009; Wu *et al.* 2009; Yue & Xu, 2015) and EGTA-resistant endocytosis following $depol_{50msX10}$, ATP-independent endocytosis did not involve acute maturation of clathrin-coated pits (Fig. 4). Thus, ATP-independent endocytosis at calyces represents a novel mechanism of endocytosis that functions along with ATP-dependent endocytosis simultaneously at the same synapses, in contrast to previous reports of either ATP-dependent endocytosis (Heidelberger, 2001; Rangaraju *et al.* 2014; Pathak *et al.* 2015) or ATP-independent endocytosis (Van Hook & Thoreson, 2012). It should be noted that, as a part of ATP-dependent endocytosis, clathrin-mediated endocytosis remained in operation at intense activity (e.g. $depol_{50msX10}$) (Fig. 4) and near physiological temperature (Fig. 9), although its share in the total endocytosis decreased because clathrin-independent endocytosis, particularly ATP-independent endocytosis, became more significant.

ATP-independent endocytosis retrieves pre-existing membrane

Although ATP-independent endocytosis could contribute to compensatory endocytosis (Figs 1*C* and 7*C*), it was more dominant in excess endocytosis (Figs 1*E* and 7*A*) readily inducible by intense stimulation (Wu *et al.* 2009; Xue *et al.* 2012; Okamoto *et al.* 2016) and at elevated temperature (Renden & von Gersdorff, 2007). Two lines of evidence suggest that ATP-independent endocytosis retrieves pre-existing membrane. First, ATP-independent endocytosis was abolished by EGTA (10–20 mM), which also blocked pre-existing membrane from endocytosis (Fig. 3*A* and *E*). Second, it was not affected by reduction of exocytosis, and correlated with retrieval of pre-existing membrane in the presence of T/C (Fig. 3*E*). By contrast, ATP-dependent endocytosis was impaired by T/C (Xu *et al.* 2013) but rather resistant to EGTA (Figs 1 and 3). Taken together, ATP-independent endocytosis retrieved pre-existing membrane, whereas ATP-dependent endocytosis mainly retrieved newly fused membrane. The distinct ATP requirement could be used to distinguish membrane sources undergoing endocytosis, especially when Ca^{2+} current or exocytosis significantly changes over repetitive stimulation (Fig. 3*B*) and thus affects the accuracy of the subtraction method (Xue *et al.* 2012). As a result of experimental limitations, the present study does not exclude the possibility that the pre-existing retrievable membrane needs ATP for sorting and priming at stages much earlier (e.g. > 4 min) than Ca^{2+}-dependent initiation of its retrieval.

Retrieval of pre-existing membrane has also been demonstrated by imaging of vesicular membrane cargos, such as synaptotagmin and synaptobrevin, which pre-exist at axon surface and participate in endocytosis following a brief train of action potentials (Wienisch & Klingauf, 2006;

Hua *et al.* 2011). These pre-existing molecules are retained from previous exocytosis, and probably pre-sorted into membrane at periactive zones after dispersion from fusion sites (Hua *et al.* 2011; Gimber *et al.* 2015). Consistent with a farther location of pre-existing membrane from fusion sites and Ca^{2+} channels, ATP-independent endocytosis was preferentially blocked by EGTA (Figs 3 and 8), a slow Ca^{2+} buffer that can restrict spatial diffusion of Ca^{2+} from Ca^{2+} entry sites. ATP-dependent endocytosis of newly fused membrane was not blocked by EGTA, and should occur within the vicinity of Ca^{2+} channels (Yamashita *et al.* 2010). Because ATP-independent endocytosis was minor following mild stimulation at room temperature (Figs 1 and 2), we suggest that pre-existing membrane is less privileged in endocytosis than newly fused membrane. This suggestion contradicts a prevailing view that pre-existing membrane is preferentially retrieved by mild stimulation (Wienisch & Klingauf, 2006; Hua *et al.* 2011). The discrepancy may arise from differences in boutons, assays and experimental conditions. First, as estimated by Cm measurement from depletion tests with repetitive stimulation, pre-existing membrane at calyces is $>$ 3-fold greater than the readily releasable vesicle pool (Fig. 3) (Wu *et al.* 2009; Xue *et al.* 2012) and could respond to a large range of stimulation with graded contribution to endocytosis. Imaging at hippocampal boutons instead reports a retrievable pool equivalent to the readily releasable pool (Hua *et al.* 2011). With ∼30% of synaptotagmin and synaptobrevin expressed at the hippocampal axon surface (Granseth *et al.* 2006; Hua *et al.* 2011), whether the current measurement reflects all the pre-existing retrievable membrane remains unknown. Second, we observed significant ATP-independent endocytosis following stimulation with the mild $depol_{1msX20}$ at 34–35°C (Fig. 7*E* and *F*). This observation suggests that pre-existing membrane could be readily retrieved at physiological temperature. We were unable to test stimulation milder than $depol_{20ms}$ at room temperature or milder than $depol_{1msX20}$ at 34–35°C because block of ATP hydrolysis reduced ΔCm so severely that we could not separate endocytosis from noisy drift in Cm. In summary, the results of the present study suggest that pre-existing membrane significantly contributes to endocytosis at nerve terminals, although not as a preferential source.

ATP-independent endocytosis is modulated by nSMase

The results of the present study indicate that endocytosis of pre-existing membrane is different from ATP-dependent compensatory endocytosis, although both involve calmodulin (Wu *et al.* 2009), calcineurin, GTP and dynamin (Xue *et al.* 2012), as well as membrane cholesterol (Yue & Xu, 2015). The present study observed that inhibition of nSMase reduced ATP-independent endocytosis but not slow compensatory endocytosis (Figs 5 and 8). This suggests that, by contrast to a common role of cholesterol in multiple forms of endocytosis (Yue & Xu, 2015), SMase selectively modulates endocytosis of pre-existing membrane. SMase catalyses hydrolysis of sphingomyelin into ceramide and phosphocholine, which can be metabolized into bioactive sphingolipids. Both ceramide and sphingolipids (e.g. sphingosine-1-phosphate) have been reported to modulate endocytosis in non-neuronal cells (Chen *et al.* 1995; Shen *et al.* 2014), probably by regulating curvature generation and early stages in endocytosis. Although exposure to exogenous SMase induces significant membrane retrieval at non-neuronal cells (Zha *et al.* 1998; Rosa *et al.* 2010; Lariccia *et al.* 2011; but see also Chen *et al.* 1995), we detected variable minor effects at calyces (Fig. 6). It is probable that modulation by SMase is confined to endocytosis at specific membrane compartments, such as domains enriched with nSMase on cytosolic membrane leaflet, instead of random membrane readily accessible to exogenous SMase. Consistent with this scenario, pre-existing membrane can be depleted by repetitive stimulation (Fig. 3*A*) (Xue *et al.* 2012) and thus is distinguishable from non-retrievable surface membrane. Sphingomyelin and cholesterol may form lipid microdomains or rafts, which are transformed into ceramide-enriched rafts via activation of SMase (Bollinger *et al.* 2005). It remains to be determined whether the retrievable pre-existing membrane co-localizes with nSMase-enriched domains, and whether bioactive sphingolipids and/or ceramide-enriched rafts selectively modulate its endocytosis. Future research should also determine whether SMase-enriched domains are farther away from Ca^{2+} channels and thus require increased activity and temperature to generate sufficient Ca^{2+} elevation to induce ATP-independent endocytosis. Alternatively, we cannot exclude the possibility of underestimating the effects of exogenous SMase at calyces because of insufficient SMase exposure during minutes of dialysis or bath incubation with brain slices. Nevertheless, by observing inhibitory effects of nSMase inhibitors on endocytosis of pre-existing membrane (Figs 5 and 8), the present study provides new insights into the regulatory role of sphingolipids in endocytosis at nerve terminals (Puchkov & Haucke, 2013).

Excess endocytosis has been reported by capacitance measurements at many neurons and endocrine cells (Thomas *et al.* 1994; Artalejo *et al.* 1995; Smith & Neher, 1997; Engisch & Nowycky, 1998; Lee & Tse, 2001; Renden & von Gersdorff, 2007; He *et al.* 2008; Van Hook & Thoreson, 2012; Xue *et al.* 2012), suggesting that ATP-dependent and ATP-independent mechanisms characterized at calyces may also function simultaneously at other cells. The ATP-independent mechanism provides a critical means of recovering membrane at elevated

temperature and activity, when the consumption of cytosolic ATP is rapid (Rangaraju et al. 2014). It can efficiently retrieve membrane without competing for ATP with processes such as vesicle priming, ATP-dependent endocytosis, vesicle reacidification, actin polymerization, ion channel activity and ATP-dependent pumps. The present study did not address what membrane structures or molecules ATP-independent endocytosis retrieved because of difficulty in performing electron microscopy on single patch-clamped calyces and uncertainty with respect to fully depriving cytosolic ATP at intact calyces with the external application of blockers. Future investigations of ATP-independent endocytosis of pre-existing membrane will promote our knowledge of exocytosis-endocytosis coupling, membrane reorganization and membrane recycling at nerve terminals. To conclude, the present study highlights a less appreciated ATP-independent endocytosis, which retrieves membrane efficiently at elevated activity and near physiological temperature.

References

Arenz C & Giannis A (2000). Synthesis of the first selective irreversible inhibitor of neutral sphingomyelinase. *Angew Chem Int Ed Engl* **39**, 1440–1442.

Armbruster M & Ryan TA (2011). Synaptic vesicle retrieval time is a cell-wide rather than individual-synapse property. *Nat Neurosci* **14**, 824–826.

Artalejo CR, Henley JR, McNiven MA & Palfrey HC (1995). Rapid endocytosis coupled to exocytosis in adrenal chromaffin cells involves Ca^{2+}, GTP, and dynamin but not clathrin. *PNAS* **92**, 8328–8332.

Assaife-Lopes N, Sousa VC, Pereira DB, Ribeiro JA, Chao MV & Sebastiao AM (2010). Activation of adenosine A2A receptors induces TrkB translocation and increases BDNF-mediated phospho-TrkB localization in lipid rafts: implications for neuromodulation. *J Neurosci* **30**, 8468–8480.

Beutner D, Voets T, Neher E & Moser T (2001). Calcium dependence of exocytosis and endocytosis at the cochlear inner hair cell afferent synapse. *Neuron* **29**, 681–690.

Blasi J, Chapman ER, Yamasaki S, Binz T, Niemann H & Jahn R (1993). Botulinum neurotoxin C1 blocks neurotransmitter release by means of cleaving HPC-1/syntaxin. *EMBO J* **12**, 4821–4828.

Bollinger CR, Teichgraber V & Gulbins E (2005). Ceramide-enriched membrane domains. *Bba-Mol Cell Res* **1746**, 284–294.

Chen CS, Rosenwald AG & Pagano RE (1995). Ceramide as a modulator of endocytosis. *JBC* **270**, 13291–13297.

Cheung G & Cousin MA (2013). Synaptic vesicle generation from activity-dependent bulk endosomes requires calcium and calcineurin. *J Neurosci* **33**, 3370–3379.

de Almeida RFM, Fedorov A & Prieto M (2003). Sphingomyelin/phosphatidylcholine/cholesterol phase diagram: boundaries and composition of lipid rafts. *Biophysical J* **85**, 2406–2416.

Delvendahl I, Vyleta NP, von Gersdorff H & Hallermann S (2016). Fast, temperature-sensitive and clathrin-independent endocytosis at central synapses. *Neuron* **90**, 492–498.

Engisch KL & Nowycky MC (1998). Compensatory and excess retrieval: two types of endocytosis following single step depolarizations in bovine adrenal chromaffin cells. *J Physiol* **506**, 591–608.

Gimber N, Tadeus G, Maritzen T, Schmoranzer J & Haucke V (2015). Diffusional spread and confinement of newly exocytosed synaptic vesicle proteins. *Nat Comm* **6**, 8392.

Granseth B, Odermatt B, Royle SJ & Lagnado L (2006). Clathrin-mediated endocytosis is the dominant mechanism of vesicle retrieval at hippocampal synapses. *Neuron* **51**, 773–786.

Grundy D (2015). Principles and standards for reporting animal experiments in *The Journal of Physiology and Experimental Physiology*. *J Physiol* **593**, 2547–2549.

He Z, Fan J, Kang L, Lu J, Xue Y, Xu P, Xu T & Chen L (2008). Ca^{2+} triggers a novel clathrin-independent but actin-dependent fast endocytosis in pancreatic beta cells. *Traffic* **9**, 910–923.

Heidelberger R (2001). ATP is required at an early step in compensatory endocytosis in synaptic terminals. *J Neurosci* **21**, 6467–6474.

Holt M, Cooke A, Wu MM & Lagnado L (2003). Bulk membrane retrieval in the synaptic terminal of retinal bipolar cells. *J Neurosci* **23**, 1329–1339.

Hosoi N, Holt M & Sakaba T (2009). Calcium dependence of exo- and endocytotic coupling at a glutamatergic synapse. *Neuron* **63**, 216–229.

Hua Y, Sinha R, Thiel CS, Schmidt R, Huve J, Martens H, Hell SW, Egner A & Klingauf J (2011). A readily retrievable pool of synaptic vesicles. *Nat Neurosci* **14**, 833–839.

Jockusch WJ, Praefcke GJ, McMahon HT & Lagnado L (2005). Clathrin-dependent and clathrin-independent retrieval of synaptic vesicles in retinal bipolar cells. *Neuron* **46**, 869–878.

Kokotos AC & Cousin MA (2015). Synaptic vesicle generation from central nerve terminal endosomes. *Traffic* **16**, 229–240.

Kononenko NL & Haucke V (2015). Molecular mechanisms of presynaptic membrane retrieval and synaptic vesicle reformation. *Neuron* **85**, 484–496.

Kononenko NL, Puchkov D, Classen GA, Walter AM, Pechstein A, Sawade L, Kaempf N, Trimbuch T, Lorenz D, Rosenmund C, Maritzen T & Haucke V (2014). Clathrin/AP-2 mediate synaptic vesicle reformation from endosome-like vacuoles but are not essential for membrane retrieval at central synapses. *Neuron* **82**, 981–988.

Korinek M, Vyklicky V, Borovska J, Lichnerova K, Kaniakova M, Krausova B, Krusek J, Balik A, Smejkalova T, Horak M & Vyklicky L (2015). Cholesterol modulates open probability and desensitization of NMDA receptors. *J Physiol* **593**, 2279–2293.

Krishnan KS, Rikhy R, Rao S, Shivalkar M, Mosko M, Narayanan R, Etter P, Estes PS & Ramaswami M (2001). Nucleoside diphosphate kinase, a source of GTP, is required for dynamin-dependent synaptic vesicle recycling. *Neuron* **30**, 197–210.

Lariccia V, Fine M, Magi S, Lin MJ, Yaradanakul A, Llaguno MC & Hilgemann DW (2011). Massive calcium-activated endocytosis without involvement of classical endocytic proteins. *J Gen Physiol* **137**, 111–132.

Lee AK & Tse A (2001). Endocytosis in identified rat corticotrophs. *J Physiol* **533**, 389–405.

Lin WC, Lin CF, Chen CL, Chen CW & Lin YS (2011). Inhibition of neutrophil apoptosis via sphingolipid signaling in acute lung injury. *J Pharmacol Exp Ther* **339**, 45–53.

Lindau M & Neher E (1988). Patch-clamp techniques for time-resolved capacitance measurements in single cells. *Pflügers Arch* **411**, 137–146.

Liu B, Hassler DF, Smith GK, Weaver K & Hannun YA (1998). Purification and characterization of a membrane bound neutral pH optimum magnesium-dependent and phosphatidylserine-stimulated sphingomyelinase from rat brain. *JBC* **273**, 34472–34479.

Lou X, Paradise S, Ferguson SM & De Camilli P (2008). Selective saturation of slow endocytosis at a giant glutamatergic central synapse lacking dynamin 1. *PNAS* **105**, 17555–17560.

Maeno-Hikichi Y, Polo-Parada L, Kastanenka KV & Landmesser LT (2011). Frequency-dependent modes of synaptic vesicle endocytosis and exocytosis at adult mouse neuromuscular junctions. *J Neurosci* **31**, 1093–1105.

Mercer AJ, Szalewski RJ, Jackman SL, Van Hook MJ & Thoreson WB (2012). Regulation of presynaptic strength by controlling Ca^{2+} channel mobility: effects of cholesterol depletion on release at the cone ribbon synapse. *J Neurophysiol* **107**, 3468–3478.

Neef J, Jung S, Wong AB, Reuter K, Pangrsic T, Chakrabarti R, Kugler S, Lenz C, Nouvian R, Boumil RM, Frankel WN, Wichmann C & Moser T (2014). Modes and regulation of endocytic membrane retrieval in mouse auditory hair cells. *J Neurosci* **34**, 705–716.

Neves G & Lagnado L (1999). The kinetics of exocytosis and endocytosis in the synaptic terminal of goldfish retinal bipolar cells. *J Physiol* **515**, 181–202.

Newton AJ, Kirchhausen T & Murthy VN (2006). Inhibition of dynamin completely blocks compensatory synaptic vesicle endocytosis. *PNAS* **103**, 17955–17960.

Nguyen TH, Maucort G, Sullivan RK, Schenning M, Lavidis NA, McCluskey A, Robinson PJ & Meunier FA (2012). Actin- and dynamin-dependent maturation of bulk endocytosis restores neurotransmission following synaptic depletion. *PLoS ONE* **7**, e36913.

Okamoto Y, Lipstein N, Hua Y, Lin KH, Brose N, Sakaba T & Midorikawa M (2016). Distinct modes of endocytotic presynaptic membrane and protein uptake at the calyx of Held terminal of rats and mice. *Elife* **5**, e14643.

Pan PY, Marrs J & Ryan TA (2015). Vesicular glutamate transporter 1 orchestrates recruitment of other synaptic vesicle cargo proteins during synaptic vesicle recycling. *JBC* **290**, 22593–22601.

Pathak D, Shields LY, Mendelsohn BA, Haddad D, Lin W, Gerencser AA, Kim H, Brand MD, Edwards RH & Nakamura K (2015). The role of mitochondrially derived ATP in synaptic vesicle recycling. *JBC* **290**, 22325–22336.

Puchkov D & Haucke V (2013). Greasing the synaptic vesicle cycle by membrane lipids. *Trends Cell Biol* **23**, 493–503.

Rangaraju V, Calloway N & Ryan TA (2014). Activity-driven local ATP synthesis is required for synaptic function. *Cell* **156**, 825–835.

Renden R & von Gersdorff H (2007). Synaptic vesicle endocytosis at a CNS nerve terminal: faster kinetics at physiological temperatures and increased endocytotic capacity during maturation. *J Neurophysiol* **98**, 3349–3359.

Rosa JM, Gandia L & Garcia AG (2010). Permissive role of sphingosine on calcium-dependent endocytosis in chromaffin cells. *Pflügers Arch* **460**, 901–914.

Sankaranarayanan S & Ryan TA (2000). Real-time measurements of vesicle-SNARE recycling in synapses of the central nervous system. *Nat Cell Biol* **2**, 197–204.

Shen H, Giordano F, Wu Y, Chan J, Zhu C, Milosevic I, Wu X, Yao K, Chen B, Baumgart T, Sieburth D & De Camilli P (2014). Coupling between endocytosis and sphingosine kinase 1 recruitment. *Nat Cell Biol* **16**, 652–662.

Smith C & Neher E (1997). Multiple forms of endocytosis in bovine adrenal chromaffin cells. *J Cell Biol* **139**, 885–894.

Sun JY & Wu LG (2001). Fast kinetics of exocytosis revealed by simultaneous measurements of presynaptic capacitance and postsynaptic currents at a central synapse. *Neuron* **30**, 171–182.

Thomas P, Lee AK, Wong JG & Almers W (1994). A triggered mechanism retrieves membrane in seconds after Ca(2+)-stimulated exocytosis in single pituitary cells. *J Cell Biol* **124**, 667–675.

Torabi SF, Khajeh K, Ghasempur S, Ghaemi N & Siadat SO (2007). Covalent attachment of cholesterol oxidase and horseradish peroxidase on perlite through silanization: activity, stability and co-immobilization. *J Biotechnol* **131**, 111–120.

Trajkovic K, Hsu C, Chiantia S, Rajendran L, Wenzel D, Wieland F, Schwille P, Brugger B & Simons M (2008). Ceramide triggers budding of exosome vesicles into multivesicular endosomes. *Science* **319**, 1244–1247.

Van Hook MJ & Thoreson WB (2012). Rapid synaptic vesicle endocytosis in cone photoreceptors of salamander retina. *J Neurosci* **32**, 18112–18123.

von Gersdorff H & Borst JG (2002). Short-term plasticity at the calyx of Held. *Nat Rev Neurosci* **3**, 53–64.

von Gersdorff H & Matthews G (1994). Inhibition of endocytosis by elevated internal calcium in a synaptic terminal. *Nature* **370**, 652–655.

von Kleist L, Stahlschmidt W, Bulut H, Gromova K, Puchkov D, Robertson MJ, MacGregor KA, Tomilin N, Pechstein A, Chau N, Chircop M, Sakoff J, von Kries JP, Saenger W, Krausslich HG, Shupliakov O, Robinson PJ, McCluskey A & Haucke V (2011). Role of the clathrin terminal domain in regulating coated pit dynamics revealed by small molecule inhibition. *Cell* **146**, 471–484.

Wascholowski V & Giannis A (2006). Sphingolactones: selective and irreversible inhibitors of neutral sphingomyelinase. *Angew Chem Int Ed Engl* **45**, 827–830.

Watanabe S, Rost BR, Camacho-Perez M, Davis MW, Sohl-Kielczynski B, Rosenmund C & Jorgensen EM (2013). Ultrafast endocytosis at mouse hippocampal synapses. *Nature* **504**, 242–247.

Watanabe S, Trimbuch T, Camacho-Perez M, Rost BR, Brokowski B, Sohl-Kielczynski B, Felies A, Davis MW, Rosenmund C & Jorgensen EM (2014). Clathrin regenerates synaptic vesicles from endosomes. *Nature* **515**, 228–233.

Wienisch M & Klingauf J (2006). Vesicular proteins exocytosed and subsequently retrieved by compensatory endocytosis are nonidentical. *Nat Neurosci* **9**, 1019–1027.

Wu W, Xu J, Wu XS & Wu LG (2005). Activity-dependent acceleration of endocytosis at a central synapse. *J Neurosci* **25**, 11676–11683.

Wu XS, Lee SH, Sheng J, Zhang Z, Zhao WD, Wang D, Jin Y, Charnay P, Ervasti JM & Wu LG (2016). Actin is crucial for all kinetically distinguishable forms of endocytosis at synapses. *Neuron* **92**, 1020–1035.

Wu XS, McNeil BD, Xu J, Fan J, Xue L, Melicoff E, Adachi R, Bai L & Wu LG (2009). Ca^{2+} and calmodulin initiate all forms of endocytosis during depolarization at a nerve terminal. *Nat Neurosci* **12**, 1003–1010.

Xu J, Luo F, Zhang Z, Xue L, Wu XS, Chiang HC, Shin W & Wu LG (2013). SNARE proteins synaptobrevin, SNAP-25, and syntaxin are involved in rapid and slow endocytosis at synapses. *Cell Rep* **3**, 1414–1421.

Xu J, McNeil B, Wu W, Nees D, Bai L & Wu LG (2008). GTP-independent rapid and slow endocytosis at a central synapse. *Nat Neurosci* **11**, 45–53.

Xu J & Wu LG (2005). The decrease in the presynaptic calcium current is a major cause of short-term depression at a calyx-type synapse. *Neuron* **46**, 633–645.

Xue L, McNeil BD, Wu XS, Luo F, He L & Wu LG (2012). A membrane pool retrieved via endocytosis overshoot at nerve terminals: a study of its retrieval mechanism and role. *J Neurosci* **32**, 3398–3404.

Yamashita T, Eguchi K, Saitoh N, von Gersdorff H & Takahashi T (2010). Developmental shift to a mechanism of synaptic vesicle endocytosis requiring nanodomain Ca^{2+}. *Nat Neurosci* **13**, 838–844.

Yamashita T, Hige T & Takahashi T (2005). Vesicle endocytosis requires dynamin-dependent GTP hydrolysis at a fast CNS synapse. *Science* **307**, 124–127.

Yao L & Sakaba T (2012). Activity-dependent modulation of endocytosis by calmodulin at a large central synapse. *PNAS* **109**, 291–296.

Yim YI, Sun T, Wu LG, Raimondi A, De Camilli P, Eisenberg E & Greene LE (2010). Endocytosis and clathrin-uncoating defects at synapses of auxilin knockout mice. *PNAS* **107**, 4412–4417.

Yue HY & Xu J (2014). Myosin light chain kinase accelerates vesicle endocytosis at the calyx of Held synapse. *J Neurosci* **34**, 295–304.

Yue HY & Xu J (2015). Cholesterol regulates multiple forms of vesicle endocytosis at a mammalian central synapse. *J Neurochem* **134**, 247–260.

Zha X, Pierini LM, Leopold PL, Skiba PJ, Tabas I & Maxfield FR (1998). Sphingomyelinase treatment induces ATP-independent endocytosis. *J Cell Biol* **140**, 39–47.

Zhang Q, Li Y & Tsien RW (2009). The dynamic control of kiss-and-run and vesicular reuse probed with single nanoparticles. *Science* **323**, 1448–1453.

Additional information

Competing interests

The authors declare that they have no competing interests.

Author contributions

JX, EB and HY designed the experiments, interpreted the results and wrote the paper. HY and JX collected, assembled and analysed data. JX supervised the study. All authors approved the final version of the manuscript. The listed authors include all those who qualify for authorship.

Funding

This work has been supported by NIH grants (R01NS082759 to JX; R01AG034389-06 and 1R01NS095215-01 to EB) and by the start-up fund from Augusta University to JX.

Acknowledgements

The authors acknowledge Drs Nevin Lambert and Darrell Brann for discussions concerning the study and for their constructive comments on the manuscript.